Earth's Future

RESEARCH ARTICLE
10.1029/2022EF003011

Special Section:
CMIP6: Trends, Interactions, Evaluation, and Impacts

Future Changes in Climate and Hydroclimate Extremes in East Africa

S. H. Gebrechorkos[1], M. T. Taye[2], B. Birhanu[3], D. Solomon[4], and T. Demissie[4,5]

[1]School of Geography and Environmental Sciences, University of Southampton, Southampton, UK, [2]International Water Management Institute (IWMI), Addis Ababa, Ethiopia, [3]School of Earth Sciences, Addis Ababa University, Addis Ababa, Ethiopia, [4]International Livestock Research Institute (ILRI), Addis Ababa, Ethiopia, [5]NORCE Norwegian Research Center, Bjerknes Center for Climate Research, Bergen, Norway

Key Points:

- Precipitation, precipitation extremes, and temperature will increase in large parts of East Africa in the 21st century
- Hydrological extremes (droughts and floods) will increase in the future in large parts of Ethiopia, Kenya, and Tanzania
- Site-specific adaptation measures are urgently required to minimize the adverse impact of hydroclimate extremes in East Africa

Supporting Information:

Supporting Information may be found in the online version of this article.

Correspondence to:

S. H. Gebrechorkos,
S.H.Gebrechorkos@soton.ac.uk

Citation:

Gebrechorkos, S. H., Taye, M. T., Birhanu, B., Solomon, D., & Demissie, T. (2023). Future changes in climate and hydroclimate extremes in East Africa. *Earth's Future*, *11*, e2022EF003011. https://doi.org/10.1029/2022EF003011

Received 30 JUN 2022
Accepted 18 JAN 2023

Abstract Climate change is affecting the agriculture, water, and energy sectors in East Africa and the impact is projected to increase in the future. To allow adaptation and mitigation of the impacts, we assessed the changes in climate and their impacts on hydrology and hydrological extremes in East Africa. We used outputs from seven CMIP-6 Global Climate Models (GCMs) and 1981–2010 is used as a reference period. The output from GCMs are statistically downscaled using the Bias Correction-Constructed Analogs with Quantile mapping reordering method to drive a high-resolution hydrological model. The Variable Infiltration Capacity and vector-based routing models are used to simulate runoff and streamflow across 68,300 river reaches in East Africa. The results show an increase in annual precipitation (up to 35%) in Ethiopia, Uganda, and Kenya and a decrease (up to 4.5%) in Southern Tanzania in the 2050s (2041–2070) and 2080s (2071–2100). During the long rainy season (March–May), precipitation is projected to be higher (up to 43%) than the reference period in Southern Ethiopia, Kenya, and Uganda but lower (up to −20%) in Tanzania. Large parts of Kenya, Uganda, Tanzania, and Southern Ethiopia show an increase in precipitation (up to 38%) during the short rainy season (October–December). Temperature and evapotranspiration will continue to increase in the future. Further, annual and seasonal streamflow and hydrological extremes (droughts and floods) are projected to increase in large parts of the region throughout the 21st century calling for site-specific adaptation.

1. Introduction

The recent assessments of the Intergovernmental Panel on Climate Change (IPCC) have shown that the last four decades have been successively warmer than any decade that preceded it since 1850 with larger surface temperature increase inland due to human-influenced climate change (Masson-Delmotte et al., 2021). Climate change and variability are not anymore a future matter rather it is already affecting many regions in the world. Africa, in particular, is the most vulnerable region due to its limited adaptation capacity (Almazroui et al., 2020; IPCC, 2014; Niang et al., 2014; Sutton et al., 2011). Under the continuing change in climate, achieving water and food security and environmental sustainability require local scale and effective adaptation measures and development programmes (AghaKouchak et al., 2015; Haile et al., 2020). East Africa is one of the hot spot locations where the impact of climate change is causing devastating consequences to the livelihoods of communities in terms of food and water insecurity and impacting major sectors that contribute to the economic growth of the region (Haile et al., 2020; Omambia et al., 2012). The region is prone to droughts and floods due to high climate variability and experiences water stress due to unreliable and insufficient rainfall (Niang et al., 2014; WWF, 2006).

In Sub-Saharan Africa, as a consequence of the change and variability in climate, poor management of environmental resources (e.g., water and soil), and availability of limited information and technologies, the productivity of agricultural lands is very low. In East Africa, agriculture is the main sector for food security of more than 80% of the population and provides a significant contribution (~42%) to the region's economy (FAO, 2014). Most of the agricultural land in East Africa is owned by smallholder producers, providing about 90% of the region's agricultural production. This makes the region more susceptible to changes and variability in climate due to the farmer's limited knowledge, up-to-date information, and capacity to adapt to the changes (Kotir, 2011; Salami et al., 2010). The vulnerability of the region to climate change will be higher in the future due to the projected changes in rainfall patterns. The implication of the future change in climate to the most important sectors in the region such as agriculture, water and food will be immense (Mahoo et al., 2013; Nicol et al., 2015). In East

Africa and globally, future projections in climate show high variability in rainfall and an increase in maximum and minimum temperature which might lead to an increase in extreme events such as floods, droughts, and heavy rainstorms (Girvetz et al., 2019; IPCC, 2013; Niang et al., 2014).

Famine Early Warning Systems Network estimated millions of food-insecure people in areas suffering from drought in different seasons and locations of eastern Africa. For example, the strong 2015/2016 El Niño impacted Ethiopia and put more than 10 million people at risk (OCHA, 2016). Consecutive droughts during the short (October to December) and long rainy (March to May) seasons affected countries such as Kenya and Tanzania (Funk et al., 2018). Several studies show declining March to May rains (Gebrechorkos, Hülsmann, et al., 2019a; Liebmann et al., 2014; Lyon & DeWitt, 2012; Nicholson, 2017; W. Yang et al., 2014), which is causing consecutive droughts and impact on the environment and food security. Droughts have devastating long-term impacts on water availability and agricultural production. Given that the major livelihood is agriculture, water availability is an important factor for sustainable food production and food security in rural communities. However, due to climate variability and change, temporal and spatial change in water availability is being observed with an erratic distribution of rainfall over the growing season of crops. To assist communities to adapt to the changes in climate, it is necessary to identify the areas with communities at risk of water and food insecurity. This will be mainly related to water management for agriculture. This is because climate change will alter the demand and availability of water for agriculture, which requires sustainable adaptation measures and water management systems. While a number of studies in the region (e.g., Emiru et al., 2022; Gebrechorkos, Bernhofer, et al., 2019; Nigatu et al., 2016; Taye et al., 2018) explore the impact of climate change on water resources but they are confined to a catchment and basin scale. In addition, the studies are based on previous climate projections (e.g., Coupled Model Intercomparison Project Phase 5). The objective of this study is, therefore, to assess future changes in climate and climate extremes and their possible impacts on hydrology and hydrological extremes (floods and droughts) using the CMIP6 (Coupled Model Intercomparison Project Phase 6) projections in East Africa.

Assessing the impact of future climate requires high spatial and temporal resolution climate data synthesized from Global Climate Models (GCMs) to drive impact assessment models (Gachon & Dibike, 2007; Gebrechorkos, Hülsmann, et al., 2019b; Wilby & Dawson, 2013). GCMs are vital for understanding the global climate and assessing variability in large-scale climate variables at a global scale (IPCC, 2013; Shiogama et al., 2021). However, GCMs face large uncertainties and biases due to their mathematical formulation, spatial resolution, initial condition and forcings, and model calibration processes, which limits their application in regional and local scale impact assessment studies (Chen et al., 2011; Kamruzzaman et al., 2021; N. Khan et al., 2018; Northrop, 2013; Salman et al., 2018). To bridge the spatial resolution gap between impact assessment models and GCMs, downscaling techniques (dynamical and statistical) have been developed (Coulibaly et al., 2005; Wilby et al., 2004). Dynamical downscaling models use local physical factors (e.g., topography) to develop high-resolution climate data from GCMs. However, due to the complexity, computational resource requirement, and bias and uncertainties of the dynamical models, their application in local scale impact assessment is limited (Brown et al., 2008; Hamlet et al., 2010). Compared to dynamical models, statistical downscaling models are computationally efficient and effective methods to produce high-resolution plausible climate scenarios from GCMs (Gebrechorkos, Hülsmann, et al., 2019b; Salathe et al., 2007; Werner & Cannon, 2016; Wilby & Dawson, 2013). In addition, statistical methods face lower biases and errors, which becomes suitable for local-scale impact studies (Brown et al., 2008; Gebrechorkos, Hülsmann, et al., 2019b; M. S. Khan & Coulibaly, 2009; Wilby & Dawson, 2013).

In this study, a novel statistical downscaling model (Bias Correction-Constructed Analogs with Quantile mapping reordering, BCCAQ), capable of reproducing spatial variability and extreme events, is used to develop high-resolution historical and future climate data from the CMIP6 GCMs based on two Shared Socioeconomic Paths (SSPs). The climate data from the GCMs are used to assess changes and variability in climate and climate extremes in the region. The high-resolution downscaled climate data is used to drive a global hydrological model (Variable Infiltration Capacity, VIC) to assess the possible impact of climate change on hydrology and hydrological extremes in East Africa. This high-resolution and comprehensive assessment will provide a better understanding of the future change in climate and hydroclimate extremes (e.g., floods and droughts). In addition, it will allow the development of contextualized adaptation measures to reduce the negative impacts and improve water and food security in East Africa.

10.1029/2022EF003011

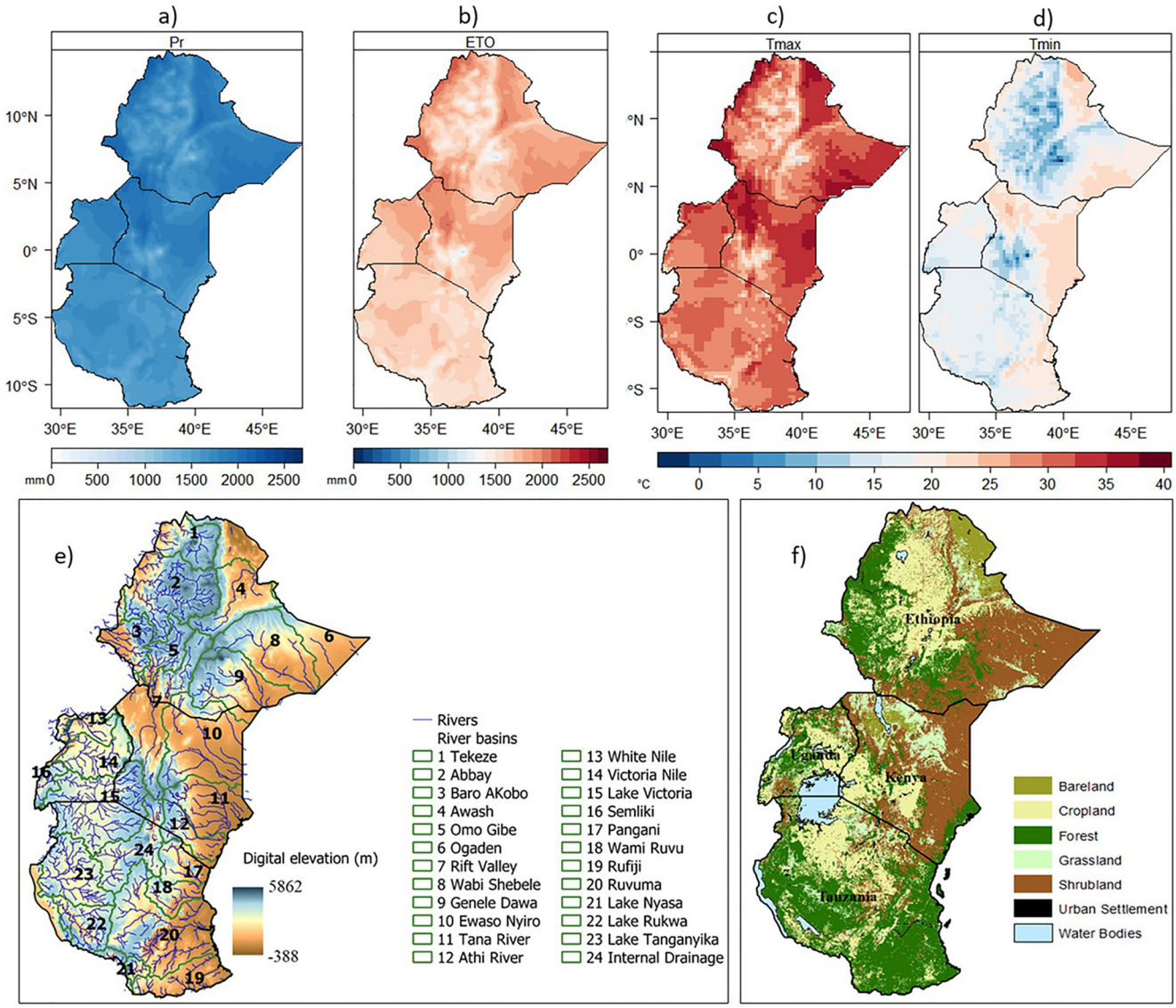

Figure 1. Annual average precipitation (Pr, mm) (a), evapotranspiration (ETO, mm) (b), and maximum (T_{max}, °C) (c) and minimum (T_{min}, °C) (d) temperature for the reference period (1981–2010). Precipitation and T_{max} and T_{min} are based on Climate Hazards Group InfraRed Precipitation with Station data (CHIRPS) and Princeton Global Meteorological Forcing Dataset (PGF), respectively. ETO is computed based on the T_{max} and T_{min} (see Section 3). The lower panel shows the elevation and basin boundaries and rivers of the 24 selected basins (e) and land use land cover map derived from the European Space Agency land cover classification map of Africa (f).

2. Study Area and Data

2.1. Study Area

The study is conducted in East Africa with a particular focus on Ethiopia, Kenya, Uganda, and Tanzania, with a very complex topography in Africa (Figure 1). Eastern Africa has one of the largest populations in Africa and it is mostly dependent on agricultural livelihoods by small-scale farmers. Tropical climate with variable precipitation modulated by the movement of the inter-tropical convergence zone (ITCZ) and varying elevation (−380 to 5,862 m, Figure 1e) characterizes this region. The annual precipitation in the region ranges from less than 100 mm to about 2,500 mm. Annual reference evapotranspiration (ETO) of the region is between 1,500 mm and more than 2,000 mm. The annual average maximum temperature (T_{max}) starts from about 25°C to about 40°C while the minimum temperature (T_{min}) ranges from less than 5°C to about 27°C. The precipitation and T_{max} and T_{min} are based on the Climate Hazards Group InfraRed Precipitation with Station data (CHIRPS; Funk et al., 2015) and Princeton Global Meteorological Forcing Dataset (PGF; Sheffield et al., 2006), respectively.

CHIRPS and PGF are the best-performing precipitation and temperature products, compared to other climate datasets such as CORDEX Regional Climate Models (RCMs) and Africa Rainfall Climatology (ARC), in East Africa (Gebrechorkos et al., 2018). The precipitation and temperature products were evaluated using several statistical methods against 332 ground station data on multiple time scales (e.g., daily and monthly) and for extreme events. The agricultural relevant seasons for the region are March to May (MAM), July to September (JAS), and October to December (OND). MAM is the major rainy season particularly in south-central and southeastern Ethiopia for pastoral and agro-pastoral livelihoods. It is also a crucial season in most of Kenya, Uganda, and Tanzania for agricultural activities. The northwestern part of Ethiopia has the JAS season as its main agricultural period, which is different from the rest of the countries. The land use land cover map is provided in Figure 1f. For hydrological analysis, 24 major river basins with average daily flow greater than 5.0 m^3/s are selected (Figure 1e).

2.2. Climate and Hydrological Data

To assess the change in climate and climate extremes and their impacts on hydrology and hydrological extremes, climate data from the CMIP6 models were used. Seven GCMs were selected for this study after evaluation of the skill of the models in East Africa (ILRI, 2021). In addition, the models were selected based on their horizontal resolution, the availability of daily data for precipitation, maximum temperature, minimum temperature, wind speed, and solar radiation. The selected models are EC-Earth3, CMCC-ESM2, GFDL-ESM4, INM-CM5, MPI-ESM1-2-LR, MRI-ESM2-0, and NorESM2-MM (Table S1 in Supporting Information S1). The global climate data from the GCMs were extracted for East Africa covering latitudes from −14.3°S to 16.5°N and longitudes from 28.0°E to 53.0°E. The future climate projections were assessed for the periods 2041–2070 and 2071–2100 representing the 2050s and the 2080s, respectively. The period from 2015 to 2040 (2020s) is only used for hydrological impact assessment. The scenarios of the future were based on the SSPs. In this study, SSP245 and SSP585 were used. SSP245 represent the medium challenges to mitigation and adaptation as well as fossil-fueled development world while SSP585 represents the high challenges to mitigation and low challenges to adaptation to climate change. In addition to the climate data, daily and monthly streamflow data from 26 stations from the Global Runoff Data Center (https://www.bafg.de/GRDC/) and the Ethiopian Ministry of Water were obtained to calibrate and validate the hydrological model.

3. Methodology

The 1981–2010 period is used as a reference to assess changes in precipitation, T_{max}, T_{min}, and reference ETO during the 2050s (2041–2070) and 2080s (2071–2100). The change in future climate is computed as a departure from the reference period. ETO is estimated using the Hargreaves method (Hargreaves & Samani, 1985), which is a suitable method for data-scare regions such as East Africa (Equation 1).

$$\mathrm{ETO} = 0.408 \times 0.0023(T_{mean} + 17.8)(T_{max} - T_{min})^{0.5} \times R_a, \quad (1)$$

where ETO is the reference crop ETO (mm day^{-1}), T_{mean} is the mean average daily temperature (°C), T_{max} and T_{min} are the daily maximum and minimum temperature (°C), respectively, and R_a is terrestrial radiation (MJ m^{-2} day^{-1}).

Further to the changes in mean precipitation, selected extreme indices related to high flows (flooding) were assessed for the historical and future periods. The extremes used here were based on the definition of the Expert Team on Climate Change Detection and Indices (Karl et al., 1999). The selected indices were the consecutive wet days (CWD), simple precipitation intensity index (SDII), maximum 5-day precipitation (Rx5day), and very wet days (R95p). The CWD and SDII are the maximum number of consecutive days with daily precipitation greater than 1 mm and the sum of daily precipitation divided by the number of wet days for a given period, respectively. The Rx5day is the maximum 5-day precipitation amount and R95p is the percentage of very wet days with precipitation greater than the 95th percentile for a given period. The GCMs have a different spatial resolution and they are bilinearly interpolated into a similar resolution (1°) for ease of computation and comparison of results. For assessing the changes in seasonal, annual, and climatological periods, the ensemble mean of GCMs was used. However, individual models are used to assess extremes. The changes in future climate are assessed by comparing to the historical period. In addition, the nonparametric Mann-Kendall test (Kendall, 1975) and Sen's slope (Sen, 1968) methods are used to assess the presence of upward and downward trends and the magnitude of change during the future climate periods, respectively.

3.1. Statistical Downscaling of GCMs and Impact Assessment

The GCMs data is statistically downscaled to drive a hydrological model to assess the impact of the projected change in climate. In this study, the novel statistical downscaling model, BCCAQ (Hiebert et al., 2018), is used to downscale daily precipitation, T_{max}, T_{min}, and wind speed from the GCMs. BCCAQ was developed at the Pacific Climate Impacts Consortium and Environment and Climate Change in Canada (https://pacificclimate.org/resources/software-library). The models, compared to other gridded statistical downscaling models such as the bias correction spatial disaggregation, climate imprint delta method, and bias-corrected climate imprint, provided a realistic estimation of hydrologic extremes (Werner & Cannon, 2016). The skill of the downscaling model depends on the quality of the reference dataset used to calibrate the model (Werner & Cannon, 2016). Hence, the best-performing climate datasets identified through an extensive evaluation (Gebrechorkos et al., 2018) for this region were used. The best-performing climate datasets for East Africa are CHIRPS (Funk et al., 2015) and PGF (Sheffield et al., 2006). The model requires a calibration period to downscale the future climate. Hence, the reference period (1981–2010) was used. The downscaling model is written in R and it is freely available at Pacific Climate Impacts Consortium (https://pacificclimate.org/resources/software-library). Finally, the downscaled daily data was used to drive a hydrological model to assess future hydrological changes in East Africa. The downscaled data from the individual models is used to drive the hydrological model. Finally, the multi-model mean is used to assess the change in the future by comparing to the reference period.

3.2. Hydrological Model and River Routing Method

The VIC (Liang et al., 1994) was used to assess the impact of the projected change in climate on the hydrology of East Africa. The VIC, semi-distributed, model computes the water and energy balance components such as ETO, infiltration, and runoff at the grid scale. The Penman-Monteith, variable infiltration curve, and nonlinear Arno-recession curve are used to compute ETO, infiltration and runoff, and baseflow simulations, respectively (Liang et al., 1994). Depending on the available soil moisture, the variable infiltration curve divides the rainfall into runoff and infiltration. VIC (version 4.2) requires daily T_{max}, T_{min}, precipitation, and wind speed. In addition, soil and vegetation parameters and vegetation library files are used to drive the model. The model is calibrated and bias-corrected at a 0.25° using station data and machine learning-derived global runoff characteristics (Beck et al., 2015) such as base flow index and different runoff percentiles (e.g., 10% and 90%) (Gebrechorkos et al., 2022; Lin et al., 2019; Y. Yang et al., 2019). The runoff characteristics were developed using more than 3,000 stations. The use of runoff characteristics maps improved model accuracy in simulating daily streamflow in data-limited catchments (Gebrechorkos et al., 2022; Lin et al., 2019). Further, the most sensitive model parameters such as the soil depth (d1–d3), VIC curve (b_{inf}), and maximum soil moisture fraction (Ds_{max}) were adjusted to match with observed streamflow.

The VIC model provides a gridded runoff and requires a routing scheme to simulate streamflow. The Routing Application for Parallel computatIon of Discharge, RAPID (David et al., 2011), a standalone runoff routing model, is used to simulate grid-based runoff to streamflow. RAPID is developed based on the Muskingum method with two main parameters (k and x) to estimate streamflow at an unprecedented number of river reaches with high efficiency (David et al., 2011). The k and x parameters are the flow travel time and a dimensionless factor (0.3), respectively, estimated for each river reach. In addition, RAPID requires a river network connectivity file, a high-resolution river network, and gridded surface and subsurface runoff output from VIC. The RAPID parameters can be computed in Arc-GIS using the python toolbox for rapid (https://github.com/Esri/python-toolbox-for-rapid). In addition, a high-resolution river network from the MERIT Hydro global hydrography datasets (Yamazaki et al., 2019) was used.

3.3. Hydrological Droughts and Floods

Daily streamflow is estimated at 67,200 river reaches in Ethiopia, Kenya, Tanzania, and Uganda during the historical (1981–2014) and future (2015–2100) periods. To assess the changes in future streamflow across the major rivers in East Africa (Figure 1e), the percentage of change is computed relative to the reference period for the 2020s (2015–2040), 2050s (2041–2070), and 2080s (2071–2100) under the two scenarios (SSP245 and SSP585). Further, the hydrological droughts (duration and severity) were assessed. The hydrological droughts were computed using a threshold-level approach. The method computes droughts events when the daily streamflow

is below a threshold value, which is computed based on a moving quantile. The threshold is defined based on the 80th percentiles of the flow duration curve from a 30-day moving window (Beyene et al., 2014; Dierauer & Whitfield, 2019). For every year of the day, the method defines a different threshold value, which is important in areas with high seasonality. The 20th percentile (i.e., flow exceeded 80% of the time) is classified as a severe hydrological drought (Rivera et al., 2017). Further, compared to other drought indices such as the standardized streamflow index (SSI), the method estimates a volume water deficit (severity) for each drought event. Further, the frequency and duration of high flows (floods) are assessed.

To assess floods, the 90th percentile (i.e., flow exceeded 10% of the time) is used as a threshold. The floods and droughts are computed for all the river reach based on the threshold. Similar to the climate extremes, the output from individual models is used to drive the hydrological model to compute the hydrological extremes (drought and floods) and the average is presented here. Finally, a set of widely used statistical measures such as the correlation coefficient and modified Kling-Gupta efficiency (KGE) (Gupta et al., 2009) are used to assess the performance of the downscaling and hydrological model.

4. Results

4.1. Changes in Precipitation and Temperature Climatology

The climatological precipitation, compared to the reference period, shows an increase during the wet season and a decrease during the dry season in Ethiopia, Kenya, Tanzania, and Uganda (Figure 2). In Ethiopia, except in January, June, and December in the 2050s, the mean precipitation shows an increase in all months by more than 4%. The increase during the long rainy season (MAM) is between 14% and 22% in the 2050s and 9%–43% in the 2080s and the maximum change is under SSP585. In Kenya, the monthly precipitation during January (up to −17%), June (up to −24%), and July (up to −23%) is lower than the reference period but it is higher during the other months. Similarly, the April–July months show a decrease in precipitation in Tanzania by more than −6.5% in the 2050s and 2080s under SSP245 and SSP585 scenarios. The June and July months also show a decrease in precipitation (−6% to 16%) in Uganda in the 2050s and 2080s. In the 2050s, precipitation in Uganda show a decrease of between −2.7% and −16% and −0.87% and −7.8% in January and December, respectively. On the other hand, T_{max} and T_{min} show an increase in Ethiopia, Kenya, Uganda, and Tanzania in the 2050s and 2080s under SSP245 and SSP585. The projected change in T_{max} and T_{min} is higher in the 2080s and under SSP585 compared to the 2050s and SSP245 (Figure 2). In Ethiopia, T_{max} and T_{min} are projected to increase by more than 0.4°C and 0.9°C in the 2050s and 2080s, respectively. In addition, the projected change in T_{max} and T_{min} in Kenya, Uganda, and Tanzania is higher than the reference period in the 2050s (0.3°C) and 2080s (1°C).

4.2. Projected Changes in Annual Precipitation, ETO, and Temperature

Future projections show an increase in annual precipitation, ETO, T_{max}, and T_{min} in the 2050s and 2080s under SSP245 and SSP585 in large parts of the region (Figures 3 and 4). Compared to the 2050s, the change is higher in the 2080s. In the 2050s, the projected change in precipitation is higher in the eastern part of Ethiopia and Kenya under SSP245 (up to 15%) and large parts of Ethiopia, Kenya, and Uganda under SSP585 (up to 29%). Similarly, in the 2080s, annual precipitation in Ethiopia, Kenya, and Uganda show an increase of up to 35%. However, in the 2050s and 2080s, the south part of Tanzania shows a decrease of up to 4.5%. Overall, the projected change in annual precipitation in Tanzania is lower compared to Ethiopia, Kenya, and Uganda.

The trend analysis also shows a significant increasing trend in Southwestern Ethiopia, Western Kenya, and Tanzania and large parts of Uganda in the 2050s under SSP245 (Figure S1 in Supporting Information S1). Under SSP585, large parts of Ethiopia, Kenya, and Uganda show a significant increasing trend (up to 12 mm/year) in the 2050s and 2080s. In line with global warming, T_{max} and T_{min} are projected to increase (up to 5.2°C) in this region, particularly higher in the 2080s under SSP585 (Figure S2 in Supporting Information S1). The projected changes for T_{max} and T_{min} for the 2050s are below 2°C for both scenarios while for the 2080s and SSP585 scenario it is projected to be higher than 3°C. In line with the projected increase in T_{max} and T_{min}, ETO is projected to increase (up to 6%) in the 2050s and 2080s (Figure 3b). In the 2050s and 2080s, the projected increase in ETO is higher in Southern Tanzania and Central Ethiopia. Unlike the other part of the region, the western part of Ethiopia shows a decrease in ETO (up to −2%) in the 2050s and 2080s under SSP585 but it will increase (up to 2%) under SSP245.

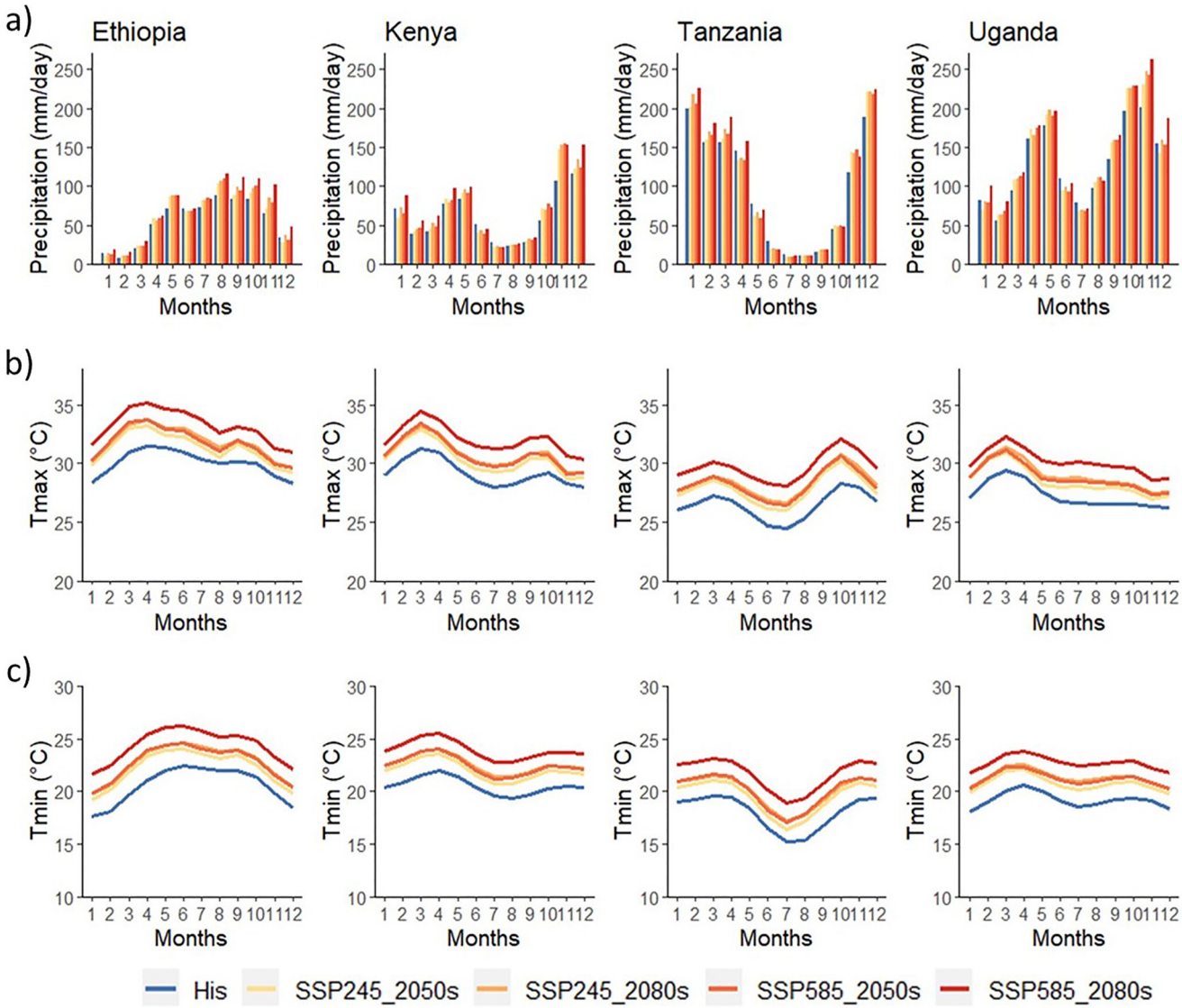

Figure 2. Climatological average precipitation (a), T_{max} (b), and T_{min} (c) for the reference period (His), 2050s and 2080s under SSP245 and SSP585 scenarios.

4.3. Seasonal Projections

Seasonal scale projections show mixed-signal, an increase and a decrease in precipitation, compared to the reference period, depending on the season and the country (Figure 4). In the 2050s and 2080s, the precipitation during MAM shows an increase (up to 43%) in large parts of Ethiopia, Kenya, and Uganda. However, in Tanzania, particularly in the southern part, the precipitation during MAM is projected to decrease (up to −20%) in the 2050s and 2080s. During JAS, the north and eastern parts of Ethiopia and western Tanzania show an increase in precipitation of up to 65%. In addition, western Kenya and Uganda also show an increase in precipitation during JAS in the 2080s. However, during JAS, the southern parts of Tanzania show a decrease (up to −20%) in precipitation in the 2080s. During the short rainy season (OND), the projection shows an increase in precipitation in large parts of Kenya, Uganda, Tanzania, and Southern and South-eastern Ethiopia. However, the northern and northeastern part of Ethiopia shows a decrease (up to −40%) during OND in the 2050s and 2080s under the two scenarios. The trend in seasonal precipitation during MAM shows an increase in the 2050s and 2080s in large parts of the region (Figure S3a in Supporting Information S1). Similarly, seasonal precipitation during OND shows an increasing trend in Ethiopia, Kenya, and Uganda and a decreasing trend in Tanzania in the 2050s and 2080s under SSP245 and SSP585. The projected increasing trend in precipitation during OND in west part of Ethiopia is statistically significant (Figure S3b in Supporting Information S1).

10.1029/2022EF003011

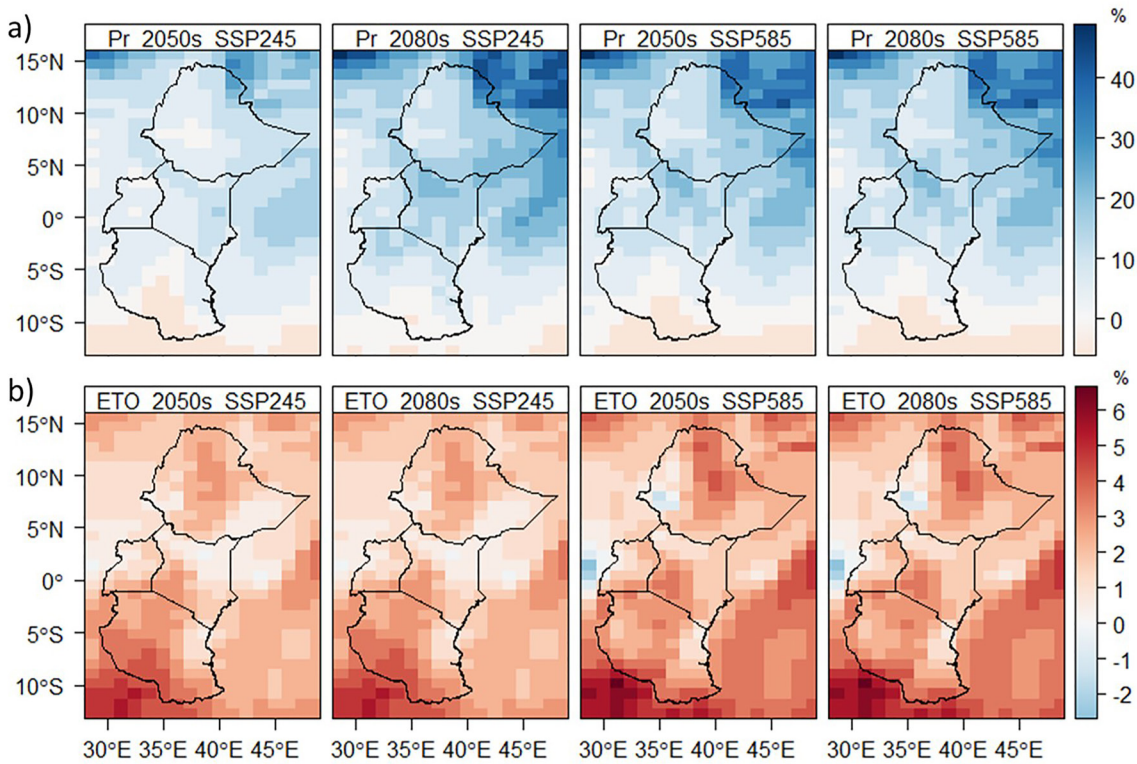

Figure 3. Projected change (%), relative to the reference period (1981–2010), in annual precipitation (Pr) (a) and ETO (b) for the 2050s and 2080s under SSP245 and SSP585 scenarios.

For ETO, increasing projection is dominant up to 15% for most places (Figure 5). The exception is the OND season which shows decreasing ETO in different parts of the region, particularly in Kenya. Compared to OND and MAM, the projected change in ETO is higher during JAS. In addition, the change is higher in the 2080s under SSP585 compared to the 2050s under SSP245. Taking the difference between the projected change in precipitation and ETO, the region shows a drying tendency compared to the reference period (Figure S4 in Supporting Information S1). During MAM and OND, there is a higher deficit in water availability in Ethiopia, Kenya, and Tanzania, compared to the reference period, in the 2050s and 2080s. However, Uganda and a few places in Western Ethiopia will be less drier in the 2050s and 2080s during MAM and OND. In addition, Lake Victoria (located at the borders of Uganda, Kenya, and Tanzania) will benefit from the projected surplus water during MAM and OND seasons. While the water deficit is higher during MAM and OND, there will be a surplus of water (up to +800 mm) in the west and northwest part of Ethiopia during JAS. On the other hand, Kenya, Uganda, and Tanzania will be much drier (up to −400 mm) than the reference period in the 2050s and 2080s under the two SSPs.

4.4. Changes in Precipitation Extremes

The number of wet days (CWD), compared to the reference period, shows an increase during MAM in Ethiopia and Kenya (up to 23%) and a decrease (up to −14%) in Tanzania (Figure 6a). In the 2050s, the northern part of Uganda show an increase (up to 5%) in CWD during MAM whereas the southern part did not show a significant change in the 2050s and 2080s under the two scenarios. Unlike the change in MAM, the western and northwestern parts of Tanzania, show a significant increase in CWD (up to 48%) during JAS. During JAS, however, CWD is projected to be lower than the reference period in the eastern and southeastern parts of Tanzania in the 2050s and 2080s (Figure 6b). Similarly, Kenya shows an increase in CWD in the central-western and a decrease in the eastern part. The OND season shows a decrease in CWD in northwestern Ethiopia but the change is lower in Uganda and Tanzania (Figure 6c). However, compared to the reference period, the eastern part of Ethiopia, particularly in the 2080s, shows an increase in CWD. Similarly, a large part of Kenya and the northwestern parts show an increase in CWD (up to 38%) in the 2050s and 2080s, respectively. Similar to the change in CWD, the Rx5day show an increase in large parts of Ethiopia, Kenya, and Uganda during MAM in the 2050s and 2080s

10.1029/2022EF003011

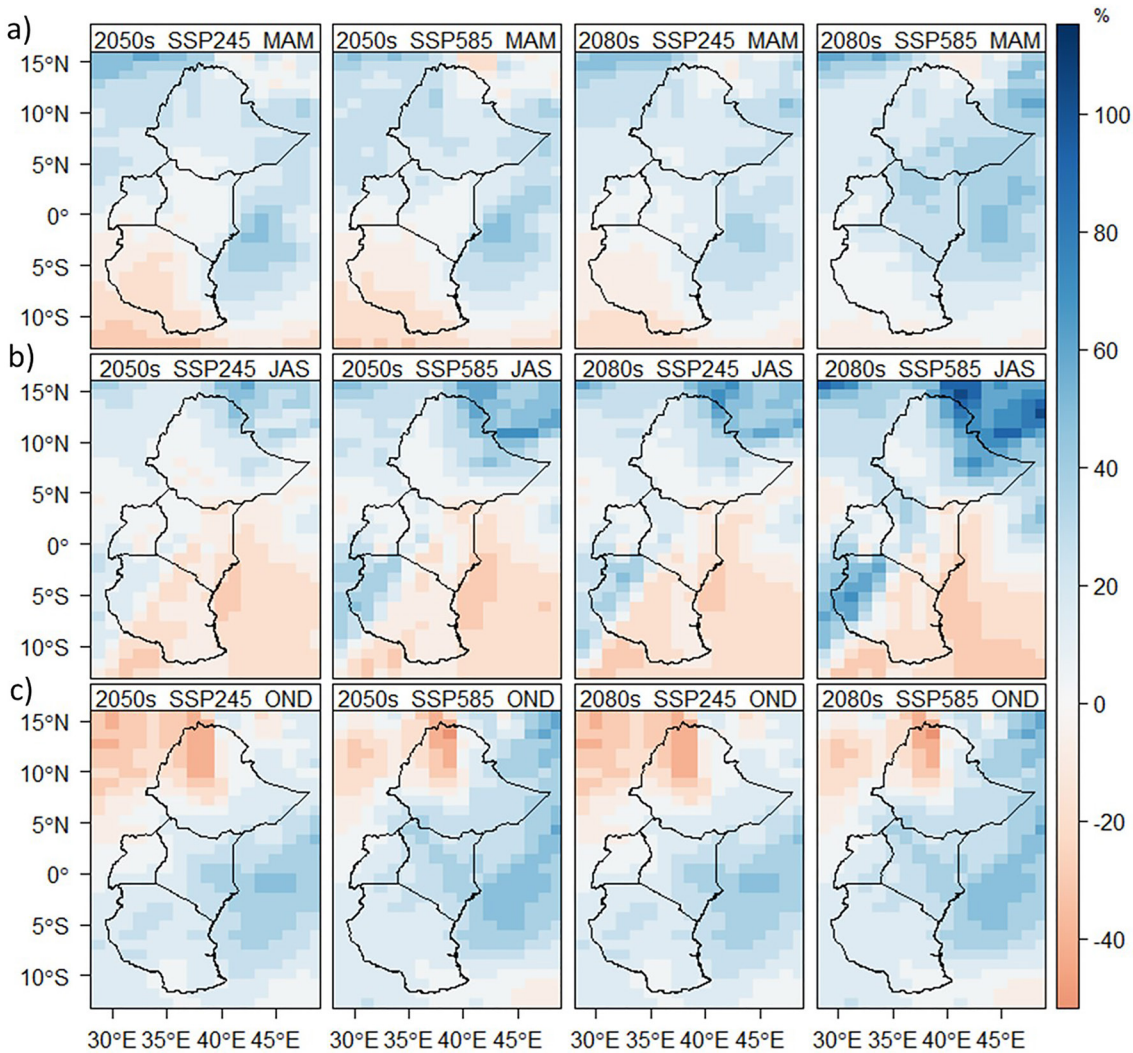

Figure 4. Seasonal changes in precipitation for Ethiopia, Kenya, Uganda, and Tanzania during MAM (a), JAS (b), and OND (c) for the 2050s and 2080s under SSP245 and SSP585 scenarios.

under the SSPs (Figure S5 in Supporting Information S1). In addition, Kenya, Uganda, Tanzania, and Southern Ethiopia show an increase in Rx5day during OND in the 2050s and 2080s. However, the Rx5day is projected to be lower than the reference period during JAS in the east part of Kenya and Tanzania. In addition, Central-Northern Ethiopia also shows a lower Rx5day compared to the reference period during OND in the 2050s under SSP245 and SSP585 and in the 2080s under SSP245.

The SDII, similar to the change in CWD, shows a mixed change in this region (Figure 7). Compared to the reference period, large parts of Ethiopia and Uganda show an increase in SDII (up to 48%) during MAM and JAS. During JAS, the west part of Kenya and Tanzania show an increase in SDII whereas a decrease in SDII is projected in Eastern Kenya and Tanzania in the 2050s and 2080s under SSP245 and SSP585. On the contrary, an increase (up to 40%) in SDII is projected during OND in Kenya, Uganda, and Tanzania in the 2050s and 2080s. In Ethiopia, while the south and southeast parts show an increase in SDII, a decrease of up to −25% is projected in central and northern parts during OND. The percentage of very wet days (R95p) did not show a significant change during MAM in this region during the 2050s and 2080s (Figure S6 in Supporting Information S1). However, during JAS a decrease in R95p is projected in different parts of western Tanzania and Kenya and an increase is projected in a few places in Tanzania (Arusha district) and northeastern Kenya. During OND, large parts of Kenya and Tanzania, show an increase in R95p of up to 60% in the 2050s and 2080s. However, in the northeastern part of Ethiopia, the R95p will be lower than the reference period in the 2050s and 2080s.

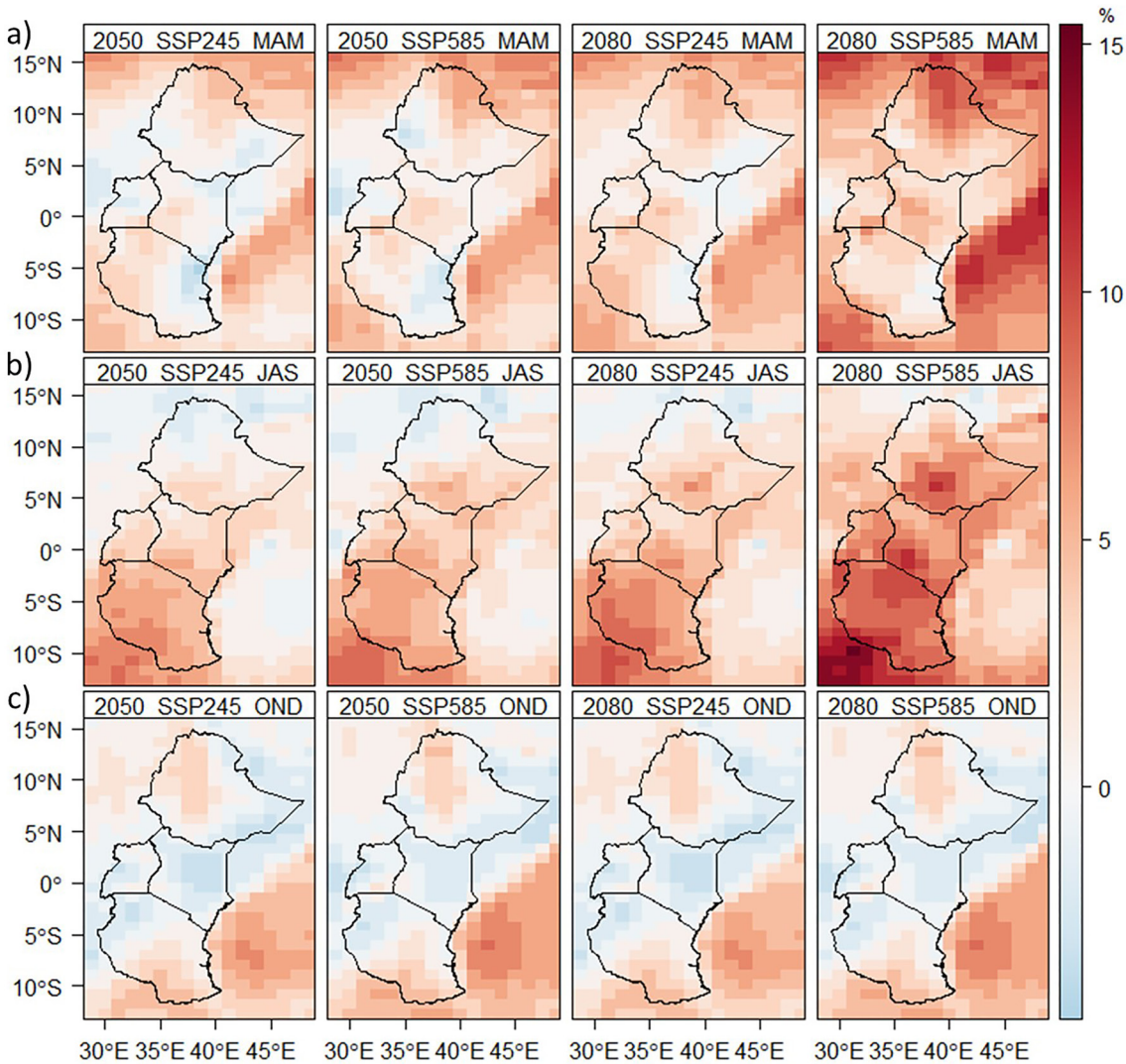

Figure 5. Seasonal changes in ETO for Ethiopia, Kenya, Uganda, and Tanzania during MAM (a), JAS (b), and OND (c) for the 2050s and 2080s under SSP245 and SSP585 scenarios.

4.5. Impact of Future Climate Change on Hydrology and Hydrological Extremes

4.5.1. Performance of the Downscaling and Hydrological Model

The downscaled daily precipitation, T_{max}, T_{min}, and wind speed are used to drive the VIC model during the historical and future (under SSP245 and SSP585) periods. The downscaling model is first assessed for its accuracy during the calibration period (1981–2010) against the observational datasets, CHIPRS for precipitation, and PGF for temperature and wind speed (Figure S7 in Supporting Information S1). The performance is higher for T_{max} and T_{min} compared to precipitation and wind speed which shows less skill in Southern Ethiopia and Western Kenya and Uganda, which show a monthly correlation of between 0.76 and 0.95 for precipitation and 0.94 to 0.97 for wind speed. The monthly correlation for T_{max} and T_{min} is higher than 0.95. In addition, the hydrological model shows KGE values between 0.48 and 0.81 during the calibration (1981–2010) and 0.39–0.67 during the validation (2011–2015) periods. In addition, the correlation ranges from 0.65 to 0.91 and 0.49–0.85 during the calibration and validation periods. The KGE values are higher at smaller to medium size basins but lower at large basins due to the large impact of water abstraction and hydraulic structures (e.g., dams) not included in the hydrological model.

10.1029/2022EF003011

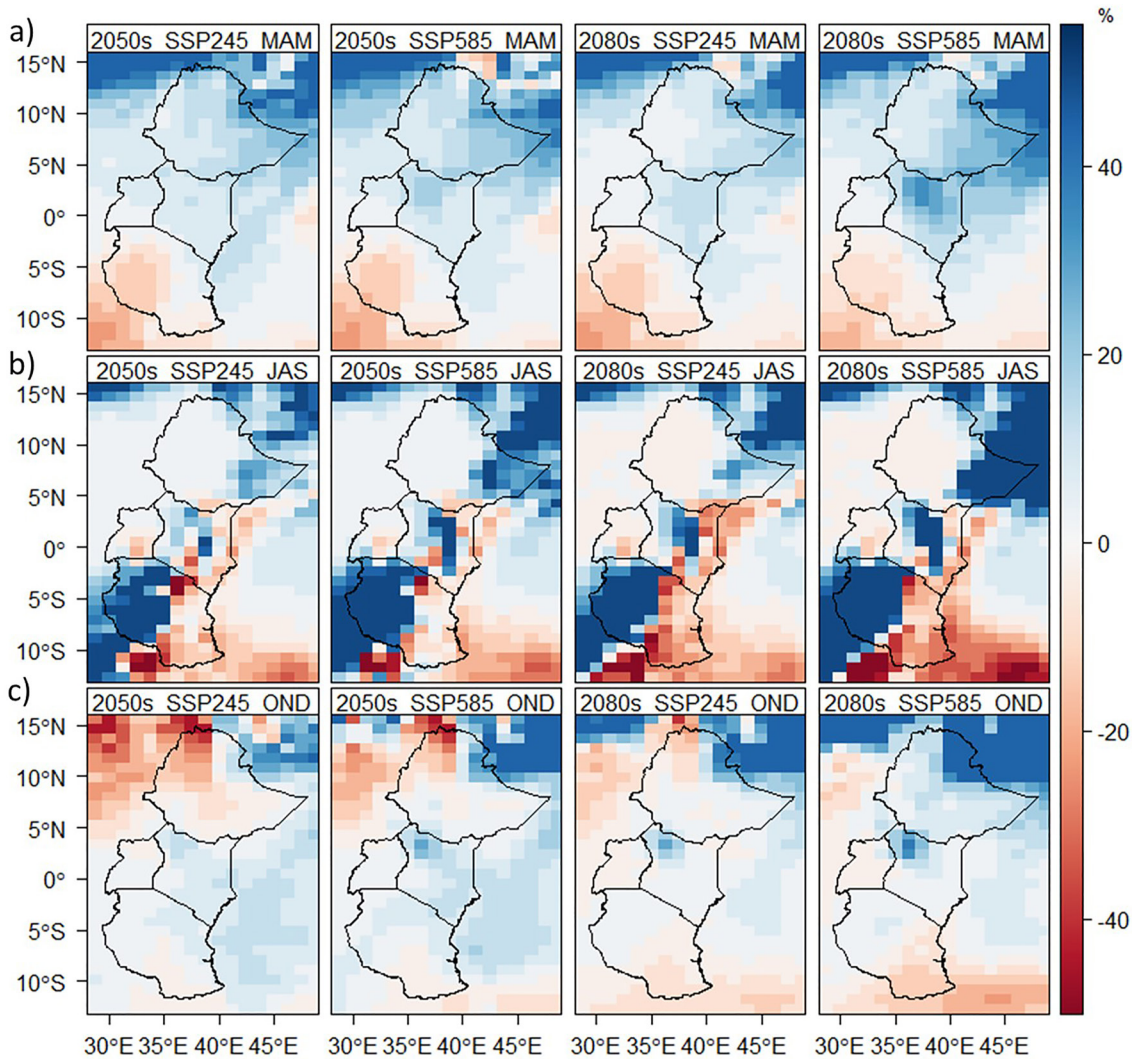

Figure 6. Percentage of change in the number of wet days (%), relative to the reference period (1981–2010), during MAM (a), JAS (b), and OND (c) for the 2050s and 2080s under SSP245 and SSP585.

4.5.2. Projected Change in Annual and Seasonal Streamflow

The projected change in annual streamflow is projected to increase in the major river basins (Figure 1e) of Ethiopia, Kenya, and Uganda in the 2020s, 2050s, and 2080s under SSP245 and SSP585 (Figure 8). In Ethiopia, the flow is projected to be lower than the reference period in Genale Dawa, Wabi Shebele, and Ogaden basins. However, the annual streamflow in the largest rivers such as Awash, Tekeze, Abbay, and Baro Akobo will increase by more than 5% throughout the 21 century. In Kenya, the major river basins such as the Tana River, Ewaso, and Athi rivers show an increase in annual flow by more than 10%, compared to the reference period, in the 2020s, 2050s, and 2080s under the two SSPs. Unlike Kenya, Ethiopia, and Uganda, the central and southern parts of Tanzania show a decrease in annual flow particularly the Rufiji Basin and upstream of the Lake Rukwa and Lake Tanganyika basins. However, the river flow at Pangani and Wami Ruvu basins will be higher (up to 25%) in the 2020s, 2050s, and 2080s under the SSPs. Similar to the basins in Kenya, the Albert Nile, Upper Nile, and Kyoga basins of Uganda will have higher annual flow in the 2020s, 2050s, and 2080s. Overall the projected increase in annual flow in the region is higher in the 2080s under SSP585 compared to the 2020s and 2050s.

Seasonally, there is an increase in streamflow during MAM and OND in Ethiopia, Kenya, and Uganda and a decrease and increase in Tanzania under SSP245 (Figure 9) and SSP585 (Figure S8 in Supporting Information S1). Similar to the projected change in annual flow, the seasonal flow during MAM is projected to increase

10.1029/2022EF003011

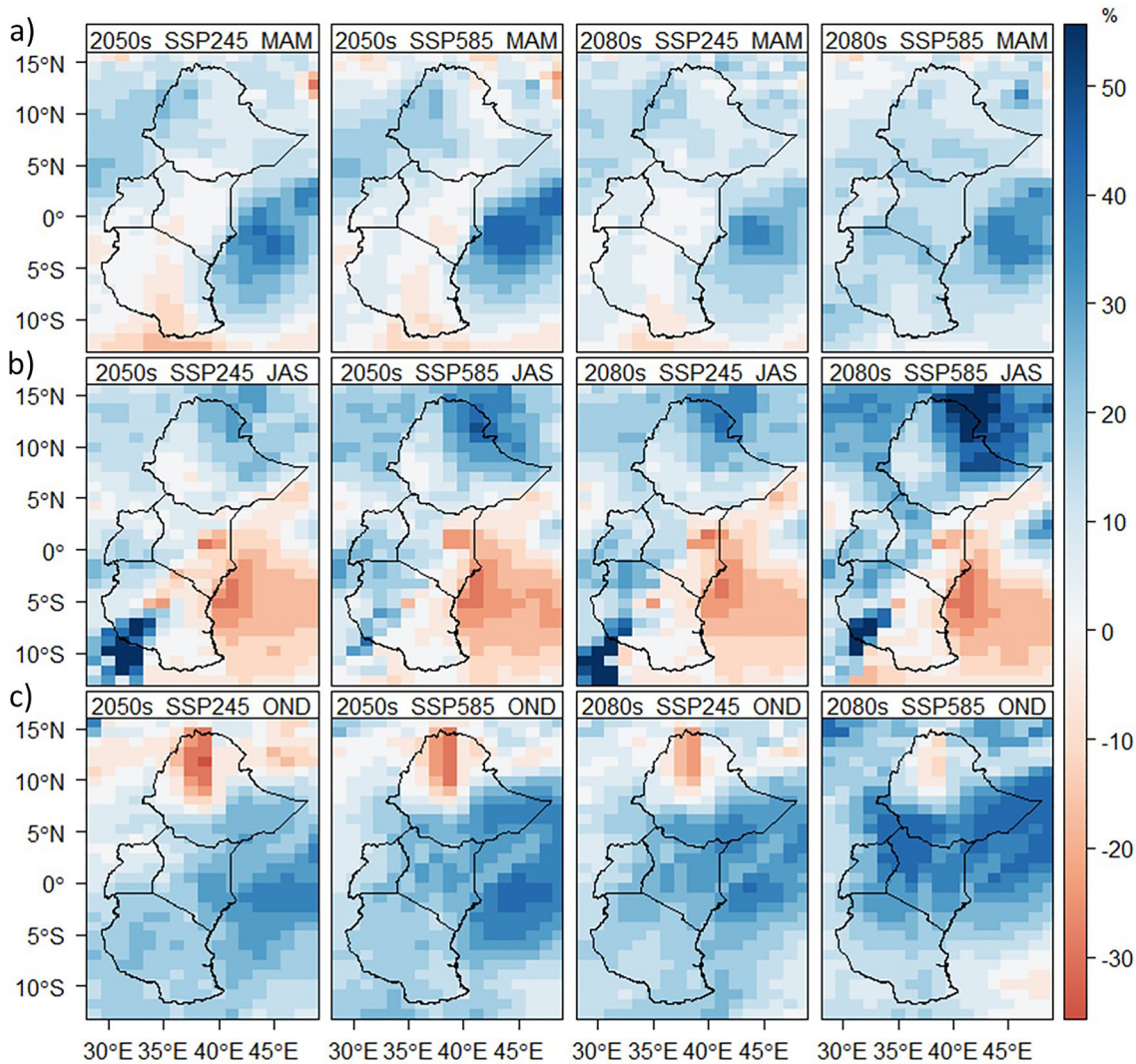

Figure 7. Percentage of change in simple precipitation intensity index (SDII, %), relative to the reference period (1981–2010), during MAM (a), JAS (b), and OND (c) for the 2050s and 2080s under SSP245 and SSP585.

in Ethiopia, Kenya, and Uganda but decrease in Tanzania. In the 2020s, the river flow in Awash and Genale Dawa basins in Ethiopia will be lower than the reference period but will increase in the 2050s and 2080s. However, the Wabi Shebele and Ogaden basins will be drier than the reference period throughout the 21 century. During MAM, the Lake Victoria, Lake Tanganyika, and Rufiji basins in Tanzania will be drier than the reference period during the 2020s, 2050s, and 2080s. On the other hand, the projected streamflow at Pangani and Ruvuma basins will be higher in the 2020s, 2050s, and 2080s. During JAS, the streamflow will be higher in all basins of Ethiopia, Kenya, and Uganda, but the Lake Victoria, Lake Tanganyika, and Rufiji basins in Tanzania will be drier in the 2020s, 2050s, and 2080s. Unlike MAM and JAS, the projected flow during the short rainy season (OND) will be higher in all basins of Tanzania, Kenya, and Uganda. Similarly, the north and south-eastern parts of Ethiopia (Awash, Tekeze, Wabi Shebele, Ogaden, Genale Dawa) will have a higher flow in the future. However, the basins in the western part of Ethiopia (Abbay and Baro Akobo) will be drier in the 2020s, 2050s, and 2080s during OND compared to the reference period.

4.5.3. Projected Change in Hydrological Drought Duration and Severity

The drought duration days tend to increase in the future in the region, particularly in Ethiopia, Kenya, and Tanzania (Figure 10). In Ethiopia, the drought days at the Tekeze, Awash, and Genale Dawa river basins will increase (up to 35%) in the 2020s, 2050s, and 2080s under the two SSPs. In addition, the drought days in Abbay,

10.1029/2022EF003011

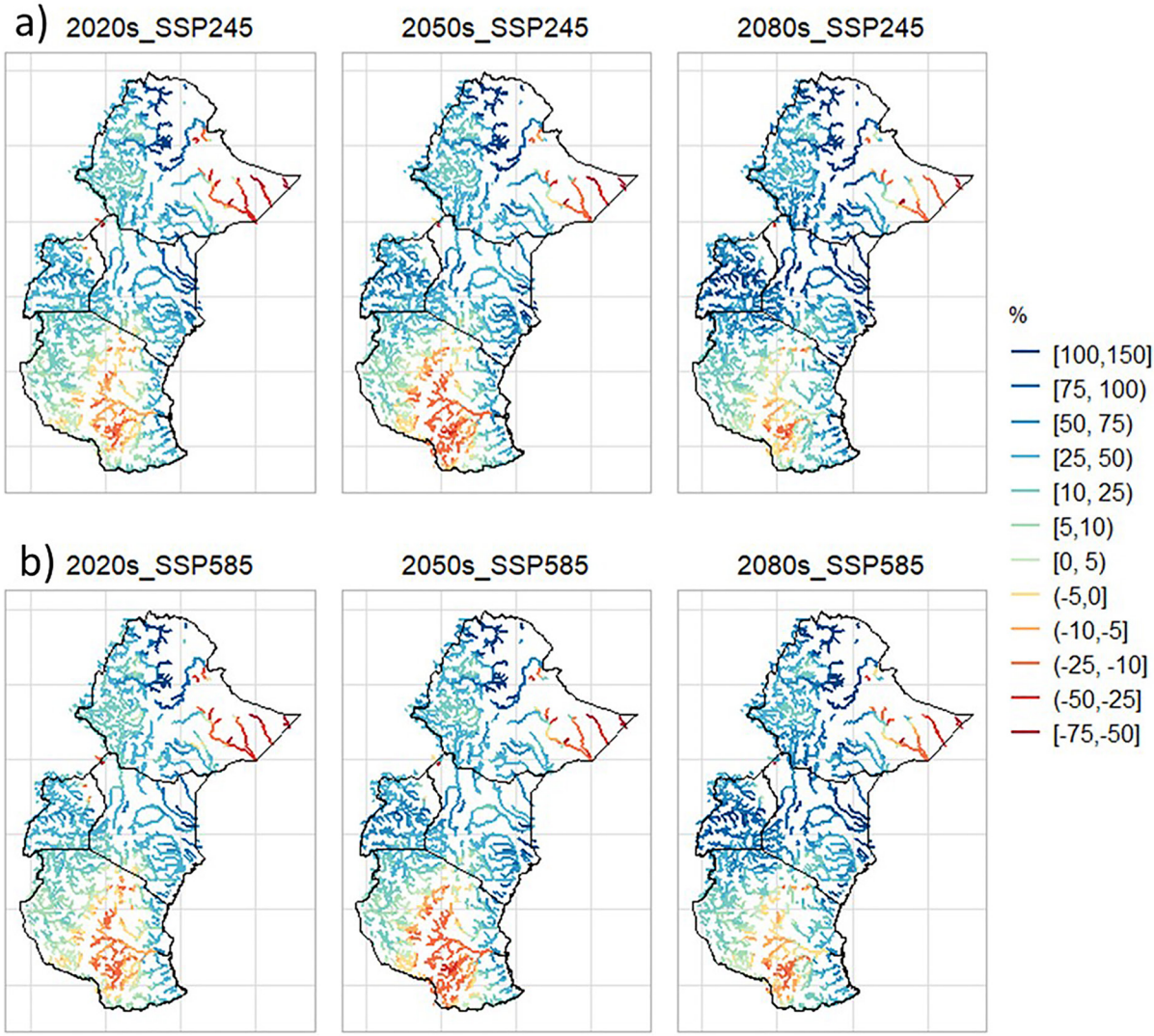

Figure 8. Projected change in annual average daily streamflow (%), relative to the reference period, for East Africa for 2020s, 2050s, and 2080s for SSP245 (a) and SSP585 (b).

Baro Akobo, and Ogaden rivers in Ethiopia will decrease in the 2080s but it is higher than the reference period in the 2020s and 2050s. The Ewaso Ngiro basin, compared to other basins, in Kenya is projected to face longer droughts throughout the 21 century. Under SSP245 and SSP585, most of the river basins in Kenya will have longer droughts in the 2050s compared to the 2020s and 2080s. Similarly, in the North part of Tanzania (Lake Victoria and Tanganyika Basins), the drought days will be longer than the reference period in the 2050s than in the 2020s and 2080s. However, drought days in the Rufiji and Wami Ruvu basins will be shorter than the reference period in the 2020s, 2050s, and 2080s. Compared to Kenya, Ethiopia, and Tanzania, the drought days in Uganda will decrease (up to −50%), particularly in the 2020s and 2080s under the SSPs. Moreover, the drought severity is projected to increase in Ethiopia and Kenya but decrease in Uganda and Tanzania (Figure S9 in Supporting Information S1). For ease of special comparison, for each river reach, the severity is normalized by their mean annual flow. The drought severity of the Awash, Wabi Shebele, Genale Dawa basins in Ethiopia will be higher than the reference period but the Abbay (in the 2050s and 2080s) and Baro Akobo (in 2080s) basins will face less severity, particularly in the 2080s. In the 2020s and 2080s, large parts of the basins in Kenya, Tanzania, and Uganda will face less severity compared to the 2050s. In the 2050s, the severity is higher in Tanzania (in Lake Tanganyika and Lake Victoria basins), Kenya (e.g., Ewaso Ngiro and Tana River) and Ethiopia (e.g., Awash, Wabi Shebele, and Genale Dawa).

10.1029/2022EF003011

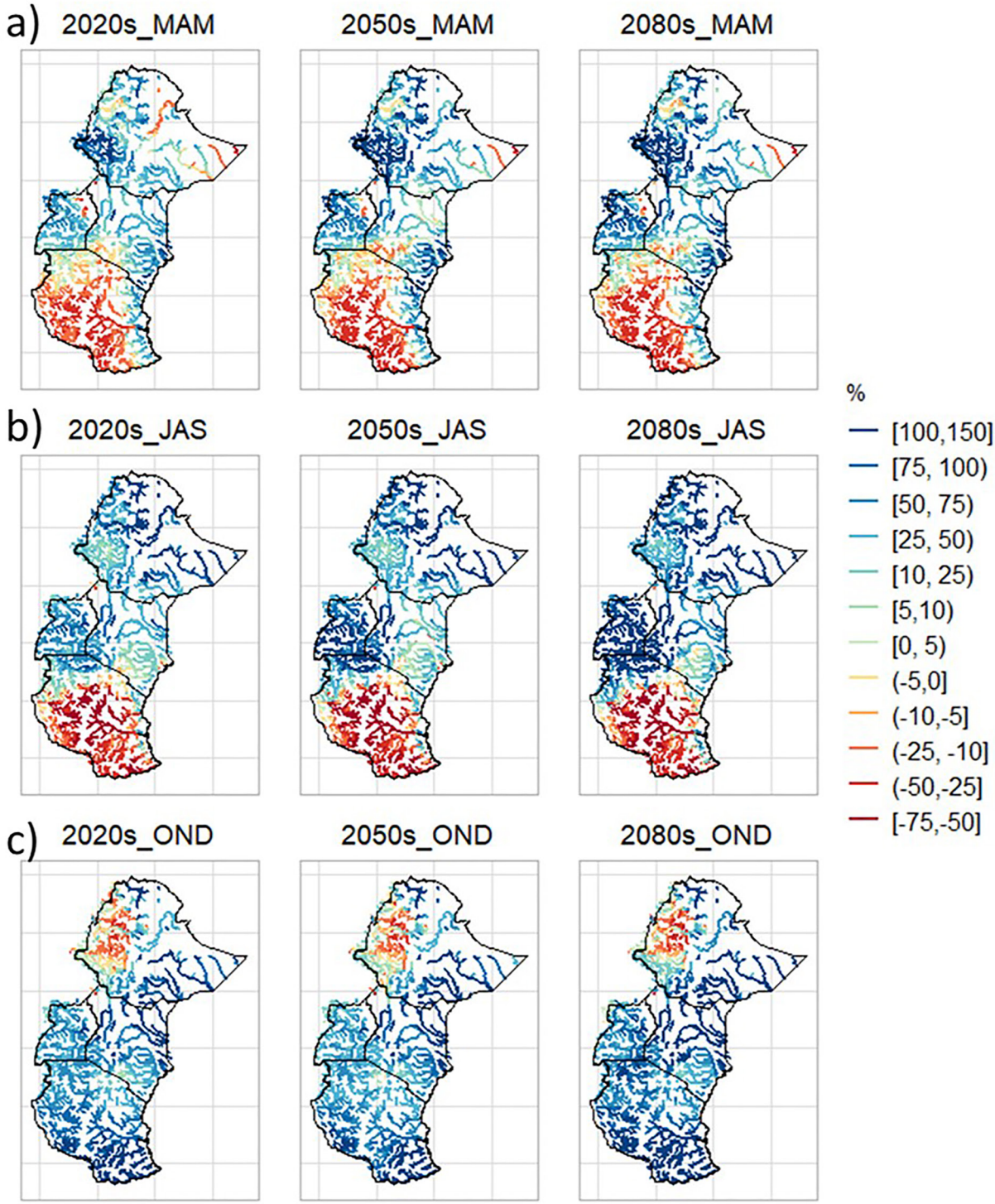

Figure 9. Projected change in seasonal streamflow (%), relative to the reference period, during MAM (a), JAS (b), and OND (c) for East Africa for the 2020s, 2050s, and 2080s under SSP245.

4.5.4. Projected Change in River Floods in Basins of East Africa

The projection also shows a significant change in the number of high flow (flood) events, particularly in the 2050s and 2080s under the SSPs (Figure 11). In the 2020s, the number of flood events is lower than the reference period in most basins of East Africa. However, the number of flood events in the 2050s and 2080s is higher (up to

10.1029/2022EF003011

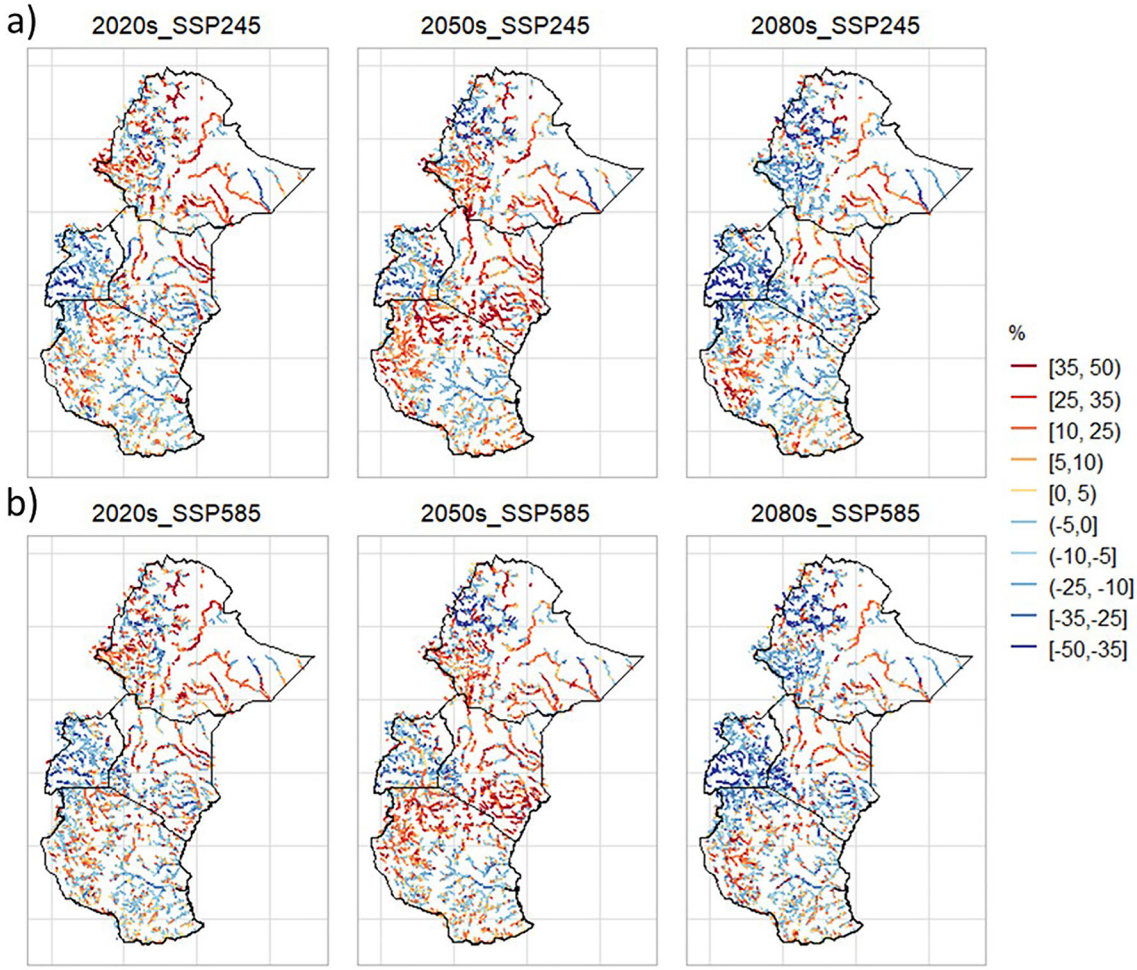

Figure 10. Projected change in drought duration days (%), relative to 1981–2010, for the 2020s, 2050s, and 2080s under SSP245 (a) and SSP585 (b).

50% per year) in the basins of Ethiopia, Kenya, and Uganda. In the 2050s and 2080s, the Tekeze and upper part of Genale Dawa and Wabi Shebele show a decrease in the number of flood events. Compared to the reference period, Lake Victoria and the north part of the Ewaso Nyiro basins in Kenya will have a lower number of flood events throughout the 21 century. Unlike other basins in East Africa, the basins in Tanzania, except Iringa, show a decrease in flood events in the 2020s, 2050s, and 2080s under the two SSPs. However, the flood events in Iringa basin in Tanzania will increase in the 2050s and 2080s by up to 50% per year. Similarly, the frequency of floods is projected to increase in the 2020s, 2050s, and 2080s (Figure 12). During the 21 century, the Abbay and Awash basins in Ethiopia will face frequent floods compared to the reference period. On the contrary, the frequency of floods in the Tekeze basin will be lower throughout the 21 century. Further, in basins of Uganda, Kenya (Tana River), and Tanzania (Iringa) an increase in the frequency of floods is projected in the 2020s, 2050s, and 2080s. Overall, the frequency and number of flood vents will increase in the future in different parts of the region under SSP245 and SSP585.

5. Discussion

Climate projections from GCMs are vital for climate change impact assessment and to develop adaptation strategies at a global and regional scale to minimize the impacts (Shiogama et al., 2021). GCMs are commonly used for historical and future climate change assessment at a global scale but cannot be directly used in regional and local scale impact assessment studies (Chen et al., 2011; Kamruzzaman et al., 2021; Khan et al., 2018; Northrop, 2013; Salman et al., 2018). Here we used a novel statistical downscaling model, BCCAQ, to downscale daily precipitation, T_{max}, T_{min}, and wind speed from seven validated CMIP6 GCMs. The GCMs and downscaled high-resolution

10.1029/2022EF003011

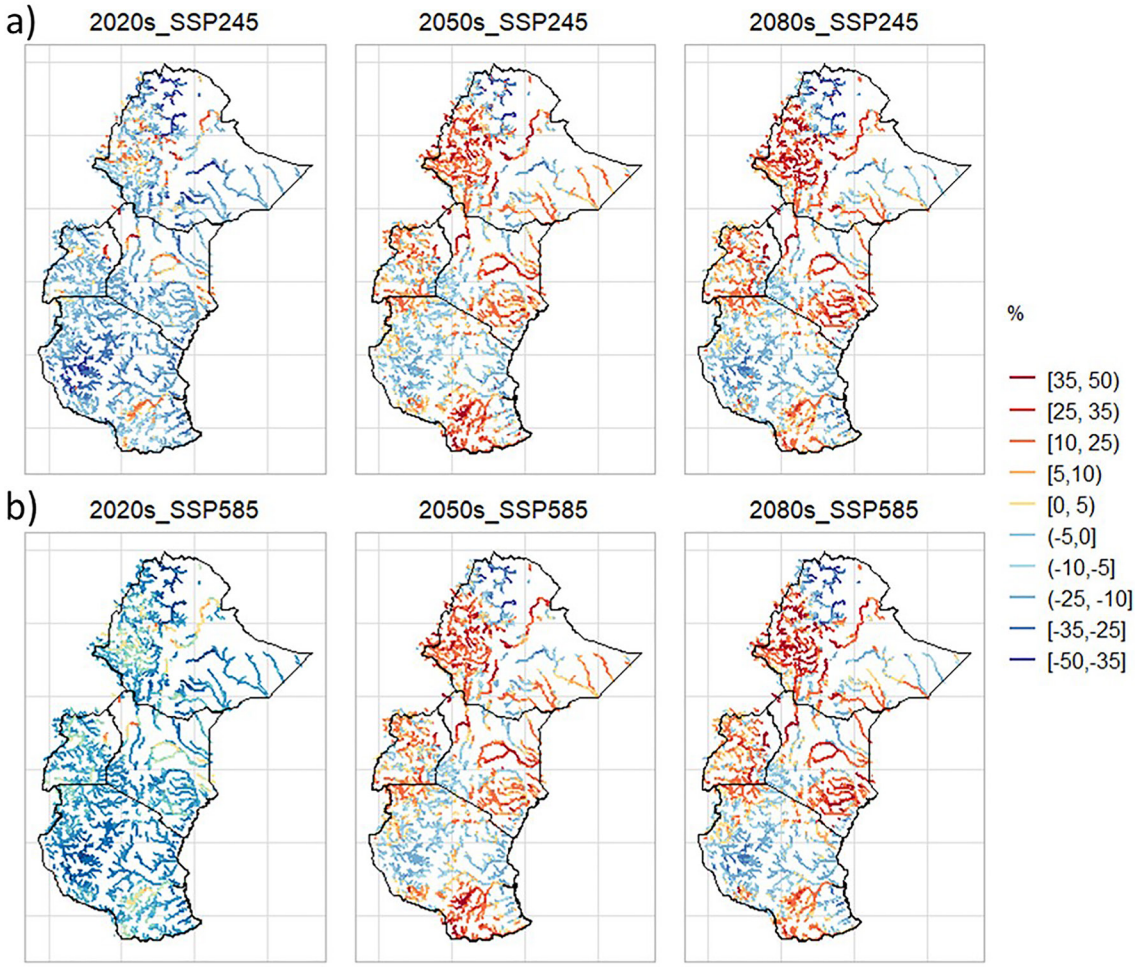

Figure 11. Projected change in number of flood events (% per year), relative to 1981–2010, for the 2020s, 2050s, and 2080s under SSP245 (a) and SSP585 (b).

(0.25°) data from the individual models are used to assess the change in climate variables and hydrology and hydrological extremes, respectively.

Based on the multimodel mean of the GCMs, the projected change in annual precipitation and temperature shows an increase in large parts of Ethiopia, Kenya, Uganda, and Tanzania in the future and this agrees with the finding of the IPCC fifth assessment report (IPCC, 2014; Niang et al., 2014). The projected change in annual temperature is higher in the 2080s under SSP585 compared to the 2050s and this is in line with previous studies based on RCMs, GCMs, and statistically downscaled GCMs (SD) covering different parts of the region (Almazroui et al., 2020; Engelbrecht et al., 2015; Gebrechorkos, Hülsmann, et al., 2019b; Getachew & Manjunatha, 2021; ICPAC, 2016; Niang et al., 2014; Osima et al., 2018). The seasonal projection shows an increase in precipitation during the long rainy season (MAM) in Ethiopia, Kenya, and Uganda in the future. However, a large part of Tanzania shows lower precipitation during MAM in the 2050s and 2080s compared to the reference period. Similar to the finding of this study, previous studies, based on the CMIP5 GCMs, SD, and RCMs, show an increase in precipitation during MAM in Ethiopia, Kenya, and Uganda and a decrease in Tanzania throughout the 21st century (Cook & Vizy, 2013; Gebrechorkos, Hülsmann, et al., 2019b; ICPAC, 2016; James & Washington, 2013; Tierney et al., 2015). According to Cook and Vizy (2013), the projected decrease in precipitation in Tanzania can be linked to the change in the climate of the Congo basins. The projected increase in precipitation during MAM appears contrary to the observed decreasing trend in the last few decades in a large part of the region (Gebrechorkos, Hülsmann, et al., 2019a; Liebmann et al., 2014; Lyon & DeWitt, 2012; Nicholson, 2017; Tierney et al., 2015; Wainwright et al., 2021; Williams & Funk, 2011). This is also known as the Eastern Africa spring rainfall paradox (Rowell et al., 2015). Similarly, during the short rainy season (OND), precipitation in

10.1029/2022EF003011

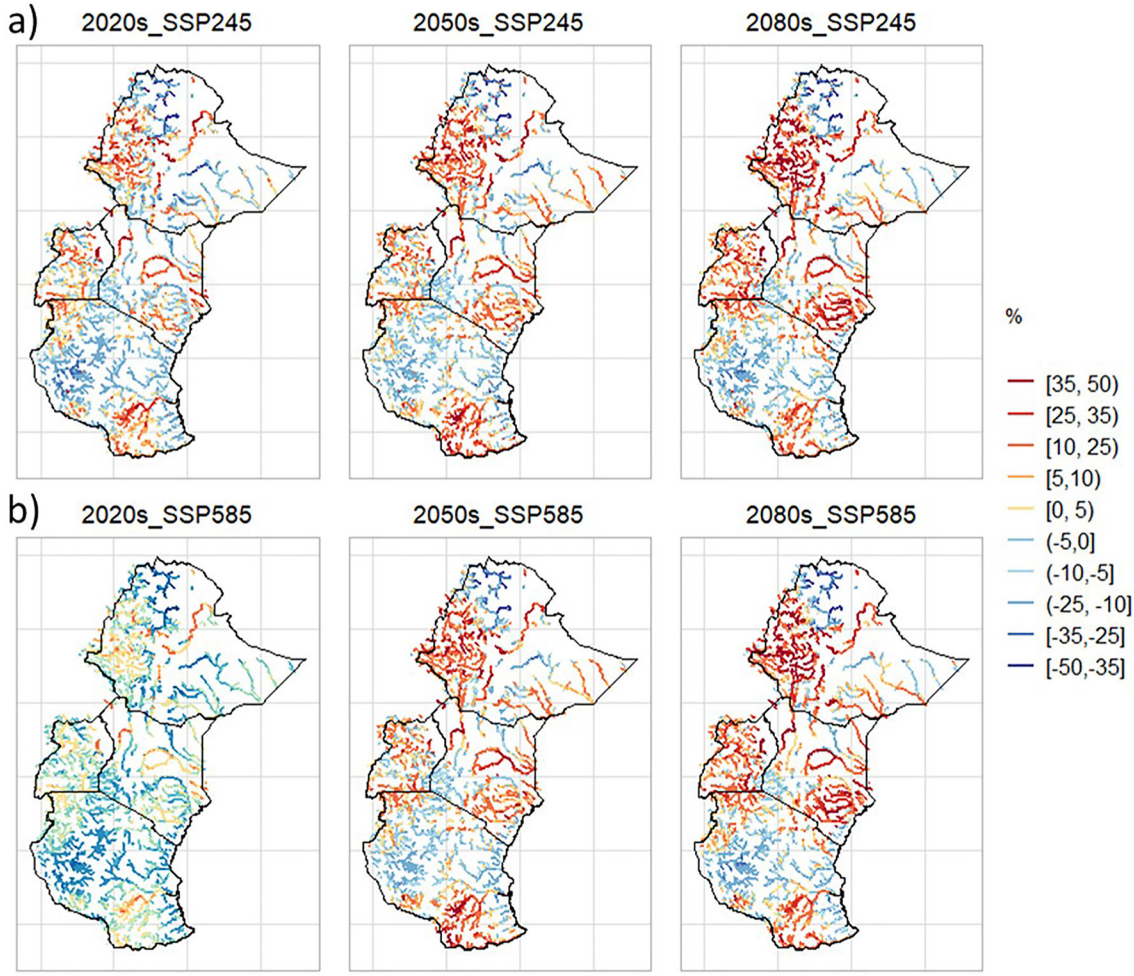

Figure 12. Projected change in frequency of flood events (%), relative to 1981–2010, for the 2020s, 2050s, and 2080s under SSP245 (a) and SSP585 (b).

Kenya, Tanzania, and Uganda is projected to increase in future. Unlike MAM, historical precipitation during OND showed an increasing trend in the last decades in East Africa (Gebrechorkos, Hülsmann, et al., 2019a; Nicholson, 2017; Rowell et al., 2015; Shongwe et al., 2011) and it is projected to increase in the future in Kenya, Uganda, and Tanzania and South and Southeastern Ethiopia.

Globally, the projected change in climate is expected to intensify the hydrological cycle leading to an increased risk and frequency of hydrological extremes such as droughts and floods (Lane & Kay, 2021; Lavers et al., 2015; Niang et al., 2014). Based on the downscaled climate data, the hydrology of the region shows a significant change in the future. Hydrological droughts (duration and severity) and floods are projected to increase in large parts of the major river basins of East Africa and this is in line with previous studies (Dai, 2012, 2013; Haile et al., 2020; Niang et al., 2014; Prudhomme et al., 2013), which presented an increase in droughts and floods in Africa and globally. The projected change in precipitation and extremes will have a significant impact on agriculture and other sectors if appropriate adaptation measures are not placed. Compared to the projected warming, the impact of change in seasonal precipitation on agriculture and the economy will be higher in East Africa.

To minimize the impact of the projected change and variability in precipitation and an increase in temperature and ETO on agriculture and other sectors, various site-specific adaptation measures are required. These are required to combat water shortages and reduce land degradation to enhance the quality and availability of water for agriculture, energy, and other sectors (Gebrechorkos et al., 2019, 2020; Gebremeskel et al., 2018; Haile et al., 2019). In agricultural intensive areas, adaptation strategies can focus on crops (e.g., crop selection, mixed cropping, soil conservation, and afforestation) and livestock (e.g., breeding strategies and management systems), labor migration, and income diversification (Akinnagbe & Irohibe, 2014; Howden et al., 2007). Calmon and

Feltran-Barbieri (2019) recommended agroforestry, integrated systems agriculture, sustainable forestry, and rehabilitation of degraded pastures as the most sustainable and effective measures to adapt to climate change and enhance the productivity of agricultural lands.

6. Summary and Conclusion

The projected change in climate and its possible impact on hydrology and hydrological extremes (floods and droughts) is assessed in East Africa using the output of selected CMIP6 GCMs. The GCMs data is statistically downscaled using a novel statistical downscaling model (BCCAQ) to drive a high-resolution hydrological model (VIC). The climate change impact on hydrology and hydrological extremes are assessed on 24 major river basins and their tributaries in East Africa.

The main findings are summarized as follows.

1. Annual precipitation is projected to increase (up to 30%) in Ethiopia, Kenya, and Uganda but decrease (up to −3%) in southern Tanzania. A similar pattern is projected during the long rainy season (MAM). On the contrary, north and northwestern Ethiopia will receive lower rainfall amounts in the future during the short rainy season (OND), whereas wetter conditions are projected for the rest of the region.
2. In line with global warming, the average temperature will continue to increase in the future under both scenarios. The increase is higher in the 2080s under SSP585 with a 1–4°C more increase than under SSP245.
3. Precipitation extremes represented by CWD, SDII, and maximum 5-day precipitation will increase in large parts of the region in the future.
4. Similar to the projected change in precipitation, annual streamflow will be higher in the basins of Ethiopia (e.g., Abbay, Awash, and Tekeze), Kenya (e.g., Ewaso Nyiro and Tana River) and Uganda (e.g., Victoria Nile) while it will decrease in Ruvuma basin in Tanzania. The projected increase in streamflow will be beneficial to the agriculture, energy, and water supply sectors.
5. Hydrological extremes (floods and droughts) are projected to increase in the future. The increase in drought duration and severity is higher in the 2050s compared to other periods, particularly in Kenya, Uganda, and Tanzania. Similarly, the magnitude and frequency of floods will increase in most basins of Ethiopia, Kenya, and Uganda but decrease in Tanzania (except in the Rufiji basin).
6. The increase in precipitation might have a positive impact on the water and agriculture sectors. However, the increase in temperature and ETO might offset water availability. Hence, site-specific adaptation strategies accounting for local heterogeneity are required.

Overall, unlike the existing adaptation strategies available in the region, an integrated approach, involving all sectors (e.g., water, energy and agriculture) and basins' scale users, is urgently required to manage the future impacts of climate change. In addition, regional capacity development and awareness about the climate and future water availability are required to sustainably manage the limited resources available in the region. Finally, considering the future variability in precipitation, a government-supported transformation from rainfed to irrigated agriculture would benefit the food security of the region.

Data Availability Statement

The data from the CMIP-6 GCMs is available at the World Climate Research Programme (WCRP, https://esgf-index1.ceda.ac.uk/projects/cmip6-ceda/). The Observational datasets, CHIRPS, and PGF can be found at Climate Hazards Center University of California, Santa Barbara (https://data.chc.ucsb.edu/products/CHIRPS-2.0/) and IRI Climate Data Library (https://iridl.ldeo.columbia.edu/SOURCES/.Princeton/.hydrology/.metdata/.NWE_Africa/.v1p0/.original/.daily/), respectively.

Acknowledgments
This work was supported by the International Development Association (IDA) of the World Bank to the Accelerating Impact of CGIAR Climate Research for Africa (AICCRA) project.

References

AghaKouchak, A., Feldman, D., Hoerling, M., Huxman, T., & Lund, J. (2015). Water and climate: Recognize anthropogenic drought. *Nature*, *524*(7566), 409–411. https://doi.org/10.1038/524409a

Akinnagbe, O. M., & Irohibe, I. J. (2014). Agricultural adaptation strategies to climate change impacts in Africa: A review. *Bangladesh Journal of Agricultural Research*, *39*(3), 407–418. https://doi.org/10.3329/bjar.v39i3.21984

Almazroui, M., Saeed, F., Saeed, S., Nazrul Islam, M., Ismail, M., Klutse, N. A. B., & Siddiqui, M. H. (2020). Projected change in temperature and precipitation over Africa from CMIP6. *Earth Systems and Environment*, *4*(3), 455–475. https://doi.org/10.1007/s41748-020-00161-x

Beck, H. E., de Roo, A., & van Dijk, A. I. J. M. (2015). Global maps of streamflow characteristics based on observations from several thousand catchments. *Journal of Hydrometeorology*, *16*(4), 1478–1501. https://doi.org/10.1175/JHM-D-14-0155.1

Beyene, B. S., Van Loon, A. F., Van Lanen, H. a. J., & Torfs, P. J. J. F. (2014). Investigation of variable threshold level approaches for hydrological drought identification. *Hydrology and Earth System Sciences Discussions*, *11*(11), 12765–12797. https://doi.org/10.5194/hessd-11-12765-2014

Brown, C., Greene, A. M., Block, P. J., & Giannini, A. (2008). *Review of downscaling methodologies for Africa climate applications*. Columbia University: International Research Institute for climate and Society. Retrieved from http://academiccommons.columbia.edu/catalog/ac:126383

Calmon, M., & Feltran-Barbieri, R. (2019). 4 ways farmers can adapt to climate change and generate income. Retrieved from https://www.wri.org/insights/4-ways-farmers-can-adapt-climate-change-and-generate-income

Chen, J., Brissette, F. P., & Leconte, R. (2011). Uncertainty of downscaling method in quantifying the impact of climate change on hydrology. *Journal of Hydrology*, *401*(3), 190–202. https://doi.org/10.1016/j.jhydrol.2011.02.020

Cook, K. H., & Vizy, E. K. (2013). Projected changes in East African rainy seasons. *Journal of Climate*, *26*(16), 5931–5948. https://doi.org/10.1175/JCLI-D-12-00455.1

Coulibaly, P., Dibike, Y. B., & Anctil, F. (2005). Downscaling precipitation and temperature with temporal neural networks. *Journal of Hydrometeorology*, *6*(4), 483–496. https://doi.org/10.1175/JHM409.1

Dai, A. (2012). Drought under global warming: A review. *Wiley Interdisciplinary Reviews: Climate Change*, 2(1), 45–65. https://doi.org/10.1002/wcc.81

Dai, A. (2013). Increasing drought under global warming in observations and models. *Nature Climate Change*, *3*(1), 52–58. https://doi.org/10.1038/nclimate1633

David, C. H., Maidment, D. R., Niu, G.-Y., Yang, Z.-L., Habets, F., & Eijkhout, V. (2011). River network routing on the NHDPlus dataset. *Journal of Hydrometeorology*, *12*(5), 913–934. https://doi.org/10.1175/2011JHM1345.1

Dierauer, J., & Whitfield, P. (2019). Daily streamflow trend and change point screening. Retrieved from https://rdrr.io/cran/FlowScreen/

Emiru, N. C., Recha, J. W., Thompson, J. R., Belay, A., Aynekulu, E., Manyevere, A., et al. (2022). Impact of climate change on the hydrology of the Upper Awash river basin, Ethiopia. *Hydrology*, *9*(1), 3. https://doi.org/10.3390/hydrology9010003

Engelbrecht, F., Adegoke, J., Bopape, M.-J., Naidoo, M., Garland, R., Marcus, T., et al. (2015). Projections of rapidly rising surface temperatures over Africa under low mitigation. *Environmental Research Letters*, *10*(8), 085004. https://doi.org/10.1088/1748-9326/10/8/085004

FAO. (2014). *The State of Food Insecurity in the world (SOFI)*. Food and Agricultural Organization of the United Nations and World Bank. Retrieved from http://www.fao.org/3/a-i4030e.pdf

Funk, C., Harrison, L., Shukla, S., Pomposi, C., Galu, G., Korecha, D., et al. (2018). Examining the role of unusually warm Indo-Pacific sea-surface temperatures in recent African droughts. *Quarterly Journal of the Royal Meteorological Society*, *144*(S1), 360–383. https://doi.org/10.1002/qj.3266

Funk, C., Peterson, P., Landsfeld, M., Pedreros, D., Verdin, J., Shukla, S., et al. (2015). The climate hazards infrared precipitation with stations—A new environmental record for monitoring extremes. *Scientific Data*, *2*(1), 150066. https://doi.org/10.1038/sdata.2015.66

Gachon, P., & Dibike, Y. (2007). Temperature change signals in northern Canada: Convergence of statistical downscaling results using two driving GCMs. *International Journal of Climatology*, *27*(12), 1623–1641. https://doi.org/10.1002/joc.1582

Gebrechorkos, S. H., Bernhofer, C., & Hülsmann, S. (2019). Impacts of projected change in climate on water balance in basins of East Africa. *Science of The Total Environment*, *682*, 160–170. https://doi.org/10.1016/j.scitotenv.2019.05.053

Gebrechorkos, S. H., Bernhofer, C., & Hülsmann, S. (2020). Climate change impact assessment on the hydrology of a large river basin in Ethiopia using a local-scale climate modelling approach. *Science of The Total Environment*, *742*, 140504. https://doi.org/10.1016/j.scitotenv.2020.140504

Gebrechorkos, S. H., Hülsmann, S., & Bernhofer, C. (2018). Evaluation of multiple climate data sources for managing environmental resources in East Africa. *Hydrology and Earth System Sciences*, *22*(8), 4547–4564. https://doi.org/10.5194/hess-22-4547-2018

Gebrechorkos, S. H., Hülsmann, S., & Bernhofer, C. (2019a). Long-term trends in rainfall and temperature using high-resolution climate datasets in East Africa. *Scientific Reports*, *9*(1), 1–9. https://doi.org/10.1038/s41598-019-47933-8

Gebrechorkos, S. H., Hülsmann, S., & Bernhofer, C. (2019b). Regional climate projections for impact assessment studies in East Africa. *Environmental Research Letters*, *14*(4), 044031. https://doi.org/10.1088/1748-9326/ab055a

Gebrechorkos, S. H., Pan, M., Lin, P., Anghileri, D., Forsythe, N., Pritchard, D. M. W., et al. (2022). Variability and changes in hydrological drought in the Volta Basin, West Africa. *Journal of Hydrology: Regional Studies*, *42*, 101143. https://doi.org/10.1016/j.ejrh.2022.101143

Gebremeskel, G., Gebremicael, T. G., & Girmay, A. (2018). Economic and environmental rehabilitation through soil and water conservation, the case of Tigray in northern Ethiopia. *Journal of Arid Environments*, *151*, 113–124. https://doi.org/10.1016/j.jaridenv.2017.12.002

Getachew, B., & Manjunatha, B. R. (2021). Climate change projections and trends simulated from the CMIP5 models for the Lake Tana subbasin, the Upper Blue Nile (Abay) River Basin, Ethiopia. *Environmental Challenges*, *5*, 100385. https://doi.org/10.1016/j.envc.2021.100385

Girvetz, E., Ramirez-Villegas, J., Claessens, L., Lamanna, C., Navarro-Racines, C., Nowak, A., et al. (2019). Future climate projections in Africa: Where are we headed? In T. S. Rosenstock, A. Nowak, & E. Girvetz (Eds.), *The climate-smart agriculture papers: Investigating the business of a productive, resilient and low emission future* (pp. 15–27). Springer International Publishing. https://doi.org/10.1007/978-3-319-92798-5_2

Gupta, H. V., Kling, H., Yilmaz, K. K., & Martinez, G. F. (2009). Decomposition of the mean squared error and NSE performance criteria: Implications for improving hydrological modelling. *Journal of Hydrology*, *377*(1), 80–91. https://doi.org/10.1016/j.jhydrol.2009.08.003

Haile, G. G., Tang, Q., Hosseini-Moghari, S.-M., Liu, X., Gebremicael, T. G., Leng, G., et al. (2020). Projected impacts of climate change on drought patterns over East Africa. *Earth's Future*, *8*(7), e2020EF001502. https://doi.org/10.1029/2020EF001502

Haile, G. G., Tang, Q., Sun, S., Huang, Z., Zhang, X., & Liu, X. (2019). Droughts in East Africa: Causes, impacts and resilience. *Earth-Science Reviews*, *193*, 146–161. https://doi.org/10.1016/j.earscirev.2019.04.015

Hamlet, A. F., Salathe, E. P., & Carrasco, P. (2010). *Statistical downscaling techniques for global climate model simulations of temperature and precipitation with application to water resources planning studies*. The Columbia Basin Climate Change Scenarios Project (CBCCSP). (Chapter 4). Retrieved from http://www.hydro.washington.edu/pub/itohver/HB2860/CBCCSP_chap4_gcm_final.pdf

Hargreaves, G., & Samani, Z. (1985). Reference crop evapotranspiration from temperature. *Applied Engineering in Agriculture*, *1*(2), 96–99. https://doi.org/10.13031/2013.26773

Hiebert, J., Cannon, A. J., Murdock, T., Sobie, S., & Werner, A. (2018). ClimDown: Climate downscaling in R. *Journal of Open Source Software*, *3*(22), 360. https://doi.org/10.21105/joss.00360

Howden, S. M., Soussana, J.-F., Tubiello, F. N., Chhetri, N., Dunlop, M., & Meinke, H. (2007). Adapting agriculture to climate change. *Proceedings of the National Academy of Sciences*, *104*(50), 19691–19696. https://doi.org/10.1073/pnas.0701890104

ICPAC. (2016). *Projected changes in rainfall and temperature over Greater Horn of Africa (GHA) in different scenarios*. IGAD Climate Prediction and Applications Centre. Retrieved from http://rcc.icpac.net/wp-content/uploads/Progress_Report_March_Hussen.pdf

ILRI. (2021). Current and future projections of flood risk and heat stress indicators over East Africa from CMIP6 models. International Livestock Research Institute (ILRI). Retrieved from https://www.ilri.org/

IPCC. (2013). Climate change 2013: The physical Science Basis. In T. F.Stocker, D. Qin, G. K. Plattner, M. Tignor, S. K. Allen, J. Boschung, A. Nauels, Y. Xia, V. Bex, & P. M. Midgley (Eds.), *WGI* (p. 1535). Cambridge Univ Press. Retrieved from http://www.ipcc.ch/report/ar5/wg1/

IPCC. (2014). *Climate change 2014 – Impacts, adaptation and vulnerability: Part B: Regional aspects: Working Group II contribution to the IPCC fifth assessment report: Volume 2: Regional Aspects*. Cambridge University Press. https://doi.org/10.1017/CBO9781107415386

James, R., & Washington, R. (2013). Changes in African temperature and precipitation associated with degrees of global warming. *Climatic Change*, *117*(4), 859–872. https://doi.org/10.1007/s10584-012-0581-7

Kamruzzaman, M., Shahid, S., Roy, D. K., Islam, A. R. T., Hwang, S., Cho, J., et al. (2021). Assessment of CMIP6 global climate models in reconstructing rainfall climatology of Bangladesh. *International Journal of Climatology*, *42*(7), 3928–3953. https://doi.org/10.1002/joc.7452

Karl, T. R., Nicholls, N., & Ghazi, A. (1999). CLIVAR/GCOS/WMO workshop on indices and indicators for climate extremes workshop summary. In T. R. Karl, N. Nicholls, & A. Ghazi (Eds.), *Weather and climate extremes: Changes, variations and a perspective from the insurance industry* (pp. 3–7). Springer Netherlands. https://doi.org/10.1007/978-94-015-9265-9_2

Kendall, M. (1975). Rank correlation measures. Retrieved from https://scholar.google.com/scholar_lookup?title=Rank+Correlation+Measures&author=Kendall,+M.G.&publication_year=1975

Khan, M. S., & Coulibaly, P. (2009). Assessing hydrologic impact of climate change with uncertainty estimates: Bayesian neural network approach. *Journal of Hydrometeorology*, *11*(2), 482–495. https://doi.org/10.1175/2009JHM1160.1

Khan, N., Shahid, S., Ahmed, K., Ismail, T., Nawaz, N., & Son, M. (2018). Performance assessment of general circulation model in simulating daily precipitation and temperature using multiple gridded datasets. *Water*, *10*(12), 1793. https://doi.org/10.3390/w10121793

Kotir, J. H. (2011). Climate change and variability in Sub-Saharan Africa: A review of current and future trends and impacts on agriculture and food security. *Environment, Development and Sustainability*, *13*(3), 587–605. https://doi.org/10.1007/s10668-010-9278-0

Lane, R. A., & Kay, A. L. (2021). Climate change impact on the magnitude and timing of hydrological extremes across Great Britain. *Frontiers in Water*, *3*. https://doi.org/10.3389/frwa.2021.684982

Lavers, D. A., Ralph, F. M., Waliser, D. E., Gershunov, A., & Dettinger, M. D. (2015). Climate change intensification of horizontal water vapor transport in CMIP5. *Geophysical Research Letters*, *42*(13), 5617–5625. https://doi.org/10.1002/2015GL064672

Liang, X., Lettenmaier, D. P., Wood, E. F., & Burges, S. J. (1994). A simple hydrologically based model of land surface water and energy fluxes for general circulation models. *Journal of Geophysical Research*, *99*(D7), 14415–14428. https://doi.org/10.1029/94JD00483

Liebmann, B., Hoerling, M. P., Funk, C., Bladé, I., Dole, R. M., Allured, D., et al. (2014). Understanding recent eastern Horn of Africa rainfall variability and change. *Journal of Climate*, *27*(23), 8630–8645. https://doi.org/10.1175/JCLI-D-13-00714.1

Lin, P., Pan, M., Beck, H. E., Yang, Y., Yamazaki, D., Frasson, R., et al. (2019). Global reconstruction of naturalized river flows at 2.94 million reaches. *Water Resources Research*, *55*(8), 6499–6516. https://doi.org/10.1029/2019WR025287

Lyon, B., & DeWitt, D. G. (2012). A recent and abrupt decline in the East African long rains. *Geophysical Research Letters*, *39*(2), L02702. https://doi.org/10.1029/2011GL050337

Mahoo, H. F., Radeny, M. A. O., Kinyangi, J., & Cramer, L. (2013). Climate change vulnerability and risk assessment of agriculture and food security in Ethiopia: Which way forward? (Working Paper). Retrieved from https://cgspace.cgiar.org/handle/10568/35082

Masson-Delmotte, V., Zhai, P., Pirani, A., Connors, S. L., Péan, C., Berger, S., et al. (Eds.). (2021). *Climate change 2021: The physical science basis. Contribution of Working Group I to the sixth assessment report of the Intergovernmental Panel on Climate Change*. Cambridge University Press.

Niang, I., Ruppel, O. C., Abdrabo, M. A., Essel, A., Lennard, C., Padgham, J., & Urquhart, P. (2014). Africa. In V. R. Barros, C. B. Field, D. J. Dokken, M. D. Mastrandrea, K. J. Mach, T. E. Bilir, et al., (Eds.), *Climate change 2014: Impacts, adaptation, and vulnerability. Part B: Regional aspects*. (WG2) (pp. 1199–1265). Cambridge University Press. Retrieved from http://www.ipcc.ch/pdf/assessment-report/ar5/wg2/WGIIAR5-Chap22_FINAL.pdf

Nicholson, S. E. (2017). Climate and climatic variability of rainfall over eastern Africa. *Reviews of Geophysics*, *55*(3), 590–635. https://doi.org/10.1002/2016RG000544

Nicol, A., Langan, S. J., Victor, M., & Gonsalves, J. F. (2015). Water-smart agriculture in East Africa. In *CGIAR research program on water, land and ecosystems*. https://doi.org/10.5337/2015.203

Nigatu, Z. M., Rientjes, T., & Haile, A. T. (2016). Hydrological impact assessment of climate change on Lake Tana's water balance, Ethiopia. *American Journal of Climate Change*, *5*(1), 27–37. https://doi.org/10.4236/ajcc.2016.51005

Northrop, P. J. (2013). Comments on "A simple, coherent framework for partitioning uncertainty in climate predictions". *Journal of Climate*, *26*(12), 4375–4376. https://doi.org/10.1175/JCLI-D-12-00527.1

Ocha. (2016). Ethiopia Weekly Humanitarian Bulletin, 16 May 2016 | HumanitarianResponse. Retrieved from https://www.humanitarianresponse.info/en/node/125848

Omambia, A. N., Shemsanga, C., & Sanchez Hernandez, I. A. (2012). Climate change impacts, vulnerability, and adaptation in East Africa (EA) and South America (SA). In W.-Y. Chen, J. Seiner, T. Suzuki, & M. Lackner (Eds.), *Handbook of climate change mitigation* (pp. 571–620). Springer US. https://doi.org/10.1007/978-1-4419-7991-9_17

Osima, S., Indasi, V. S., Zaroug, M., Endris, H. S., Gudoshava, M., Misiani, H. O., et al. (2018). Projected climate over the Greater Horn of Africa under 1.5°C and 2°C global warming. *Environmental Research Letters*, *13*(6), 065004. https://doi.org/10.1088/1748-9326/aaba1b

Prudhomme, C., Giuntoli, I., Robinson, E. L., Clark, D. B., Arnell, N. W., Dankers, R., et al. (2013). Hydrological droughts in the 21st century, hotspots and uncertainties from a global multimodel ensemble experiment. *Proceedings of the National Academy of Sciences*, *111*(9), 3262–3267. https://doi.org/10.1073/pnas.1222473110

Rivera, J. A., Araneo, D. C., & Penalba, O. C. (2017). Threshold level approach for streamflow drought analysis in the Central Andes of Argentina: A climatological assessment. *Hydrological Sciences Journal*, *62*(12), 1949–1964. https://doi.org/10.1080/02626667.2017.1367095

Rowell, D. P., Booth, B. B. B., Nicholson, S. E., & Good, P. (2015). Reconciling past and future rainfall trends over East Africa. *Journal of Climate*, *28*(24), 9768–9788. https://doi.org/10.1175/JCLI-D-15-0140.1

Salami, A., Kamara, A. B., & Brixiova, Z. (2010). *Smallholder agriculture in East Africa: Trends, constraints, and opportunities*. Africain Development Bank. Retrieved from https://www.commdev.org/smallholder-agriculture-in-east-africa-trends-constraints-and-opportunities/

Salathe, E. P., Jr., Mote, P. W., & Wiley, M. W. (2007). Review of scenario selection and downscaling methods for the assessment of climate change impacts on hydrology in the United States Pacific northwest. *International Journal of Climatology*, *27*(12), 1611–1621. https://doi.org/10.1002/joc.1540

Salman, S. A., Shahid, S., Ismail, T., Ahmed, K., & Wang, X.-J. (2018). Selection of climate models for projection of spatiotemporal changes in temperature of Iraq with uncertainties. *Atmospheric Research*, *213*, 509–522. https://doi.org/10.1016/j.atmosres.2018.07.008

Sen, P. K. (1968). Estimates of the regression coefficient based on Kendall's Tau. *Journal of the American Statistical Association*, *63*(324), 1379–1389. https://doi.org/10.1080/01621459.1968.10480934

Sheffield, J., Goteti, G., & Wood, E. F. (2006). Development of a 50-year high-resolution global dataset of meteorological forcings for land surface modeling. *Journal of Climate*, *19*(13), 3088–3111. https://doi.org/10.1175/JCLI3790.1

Shiogama, H., Ishizaki, N. N., Hanasaki, N., Takahashi, K., Emori, S., Ito, R., et al. (2021). Selecting CMIP6-based future climate scenarios for impact and adaptation studies. *Sola*, *17*(0), 57–62. https://doi.org/10.2151/sola.2021-009

Shongwe, M. E., van Oldenborgh, G. J., van den Hurk, B., & van Aalst, M. (2011). Projected changes in mean and extreme precipitation in Africa under global warming. Part II: East Africa. *Journal of Climate*, *24*(14), 3718–3733. https://doi.org/10.1175/2010JCLI2883.1

Sutton, M. A., van Grinsven, H., Billen, G., Bleeker, A., Bouwman, A. F., Bull, K., et al. (2011). Summary for policy makers. In A. Bleeker, B. Grizzetti, C. M. Howard, G. Billen, H. van Grinsven, & J. W. Erisman (Eds.), *The European nitrogen assessment: Sources, effects and policy perspectives* (pp. xxiv–xxxiv). Cambridge University Press. https://doi.org/10.1017/CBO9780511976988.002

Taye, M. T., Dyer, E., Hirpa, F. A., & Charles, K. (2018). Climate change impact on water resources in the Awash basin, Ethiopia. *Water*, *10*(11), 1560. https://doi.org/10.3390/w10111560

Tierney, J. E., Ummenhofer, C. C., & de Menocal, P. B. (2015). Past and future rainfall in the Horn of Africa. *Science Advances*, *1*(9), e1500682. https://doi.org/10.1126/sciadv.1500682

Wainwright, C. M., Finney, D. L., Kilavi, M., Black, E., & Marsham, J. H. (2021). Extreme rainfall in East Africa, October 2019–January 2020 and context under future climate change. *Weather*, *76*(1), 26–31. https://doi.org/10.1002/wea.3824

Werner, A. T., & Cannon, A. J. (2016). Hydrologic extremes – An intercomparison of multiple gridded statistical downscaling methods. *Hydrology and Earth System Sciences*, *20*(4), 1483–1508. https://doi.org/10.5194/hess-20-1483-2016

Wilby, R. L., & Dawson, C. W. (2013). The Statistical DownScaling model: Insights from one decade of application. *International Journal of Climatology*, *33*(7), 1707–1719. https://doi.org/10.1002/joc.3544

Wilby, R. L., Dawson, C. W., & Barrow, E. (2004). SDSM – A decision support tool for the assessment of regional climate change impacts. *Environmental Modelling & Software*, *17*(2), 145–157. https://doi.org/10.1016/S1364-8152(01)00060-3

Williams, A. P., & Funk, C. (2011). A westward extension of the warm pool leads to a westward extension of the Walker circulation, drying eastern Africa. *Climate Dynamics*, *37*(11–12), 2417–2435. https://doi.org/10.1007/s00382-010-0984-y

WWF. (2006). *Climate change impacts on East Africa. A review of the scientific literature*. World Wide Fund For Nature. Retrieved from https://www.wwf.or.jp/activities/lib/pdf_climate/environment/east_africa_climate_change_impacts_final.pdf

Yamazaki, D., Ikeshima, D., Sosa, J., Bates, P. D., Allen, G. H., & Pavelsky, T. M. (2019). MERIT Hydro: A high-resolution global hydrography map based on latest topography dataset. *Water Resources Research*, *55*(6), 5053–5073. https://doi.org/10.1029/2019WR024873

Yang, W., Seager, R., Cane, M. A., & Lyon, B. (2014). The East African long rains in observations and models. *Journal of Climate*, *27*(19), 7185–7202. https://doi.org/10.1175/JCLI-D-13-00447.1

Yang, Y., Pan, M., Beck, H. E., Fisher, C. K., Beighley, R. E., Kao, S.-C., et al. (2019). In quest of calibration density and consistency in hydrologic modeling: Distributed parameter calibration against streamflow characteristics. *Water Resources Research*, *55*(9), 7784–7803. https://doi.org/10.1029/2018WR024178